

Cosmological reionization simulations: all halos great and small

Ilian T. Iliev

University of Sussex

with

Garrelt Mellema (Stockholm), Paul Shapiro (Austin), Kyugjin Ahn (Chosun),
Ue-Li Pen, Dick Bond, Pat McDonald, Olivier Dore (CITA), Ben Moore, Uros Seljak,
Vincent Desjacques (Zurich), Gustavo Yepes (Madrid), Stefan Gottloeber (AIP),
Yehuda Hoffman (Jerusalem)

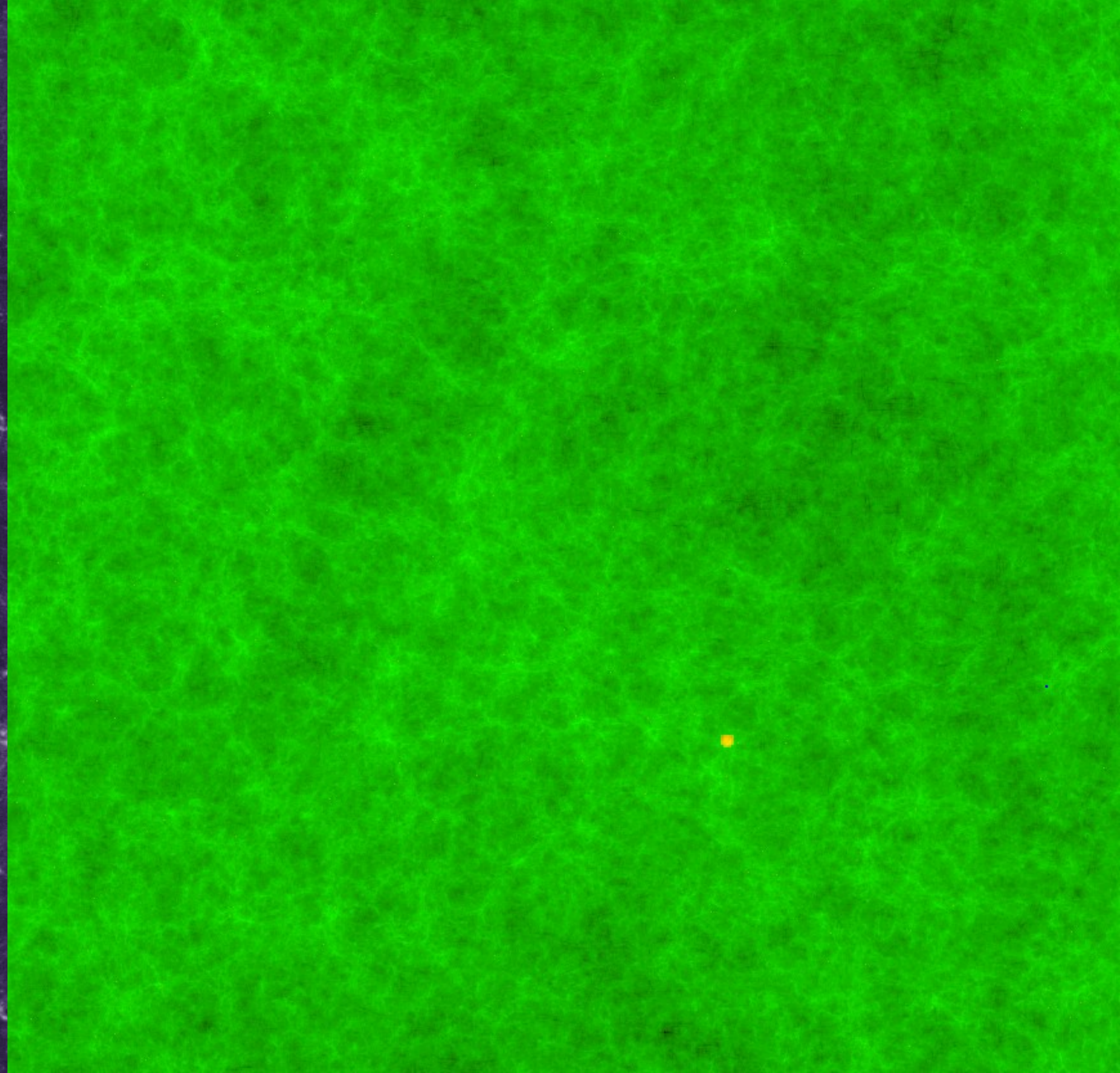
Reionization in Action: From the Dark Ages to Reionized Universe

- Strong halo clustering
- quick local percolation
- large H II regions with complex geometry.

64/h Mpc box,
WMAP3+ cosmology,
432³ radiative transfer
simulation. Evolution:
z=30 to 7.

>10⁸ solar mass halos
resolved

Simulations ran at Texas Supercomputing Center on up to 10,000 cores



EOR Simulations: High Requirements

- **Large scale** simulations: needed both **observationally** (radio observations will have multiple degree FOV) and **fundamentally** (size of HII regions >10 Mpc, long-wavelength density perturbations crucial).
- **Large dynamic range** simulations: dominant contributors to ionizing flux are **small** (dwarf and sub-dwarf) galaxies. Ideally need to resolve collapsed halos of mass $>10^8 M_{\text{solar}}$ (atomic cooling). Low dynamic range also imposes **artificial cut-offs** on density fluctuations.
- **Fast, precise** radiative transfer.

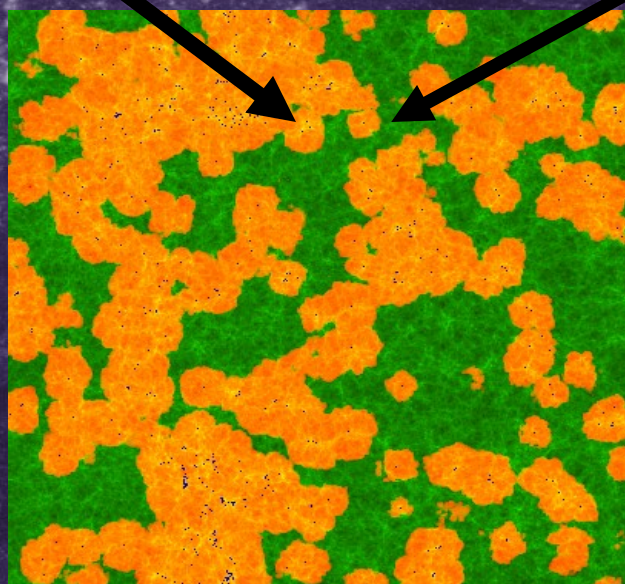
Ours are the first ever reionization simulations to satisfy these requirements. Based on them we have now produced the first realistic predictions of the EOR character and observable signatures.

Large-Scale Simulations of Reionization

[Iliev et al. 2006a, 2007a; Mellema, Iliev, et al. 2006; and in prep.]

- N-body: CubeP³M
1728³-3072³ part.
(5.2 to 29 billion) or more -
4000³-5488³ (64-165 billion)
- density slices
- velocity slices
- halo catalogues-sources
- Scales well up to 21,952
- cores

35-114/h Mpc (CubeP³M)
resolving 10⁸ M_{solar} halos
up to 21 x 10⁶ sources
50-100 dens. snapshots
simple source models
sub-grid clumping
no hydro – large scales.



- C²-Ray code
(Mellema, Iliev, et al. 2006)
- radiative transfer
 - noneq. chemistry
 - precise
 - highly efficient
 - coupled to gasdynamics
 - massively parallel (ran
on over 10,000 cores).

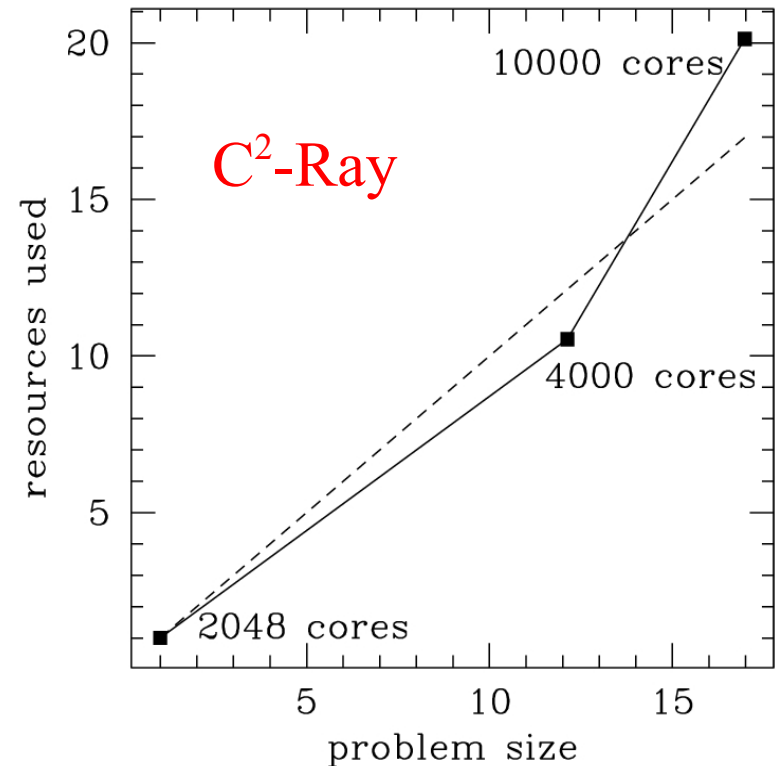
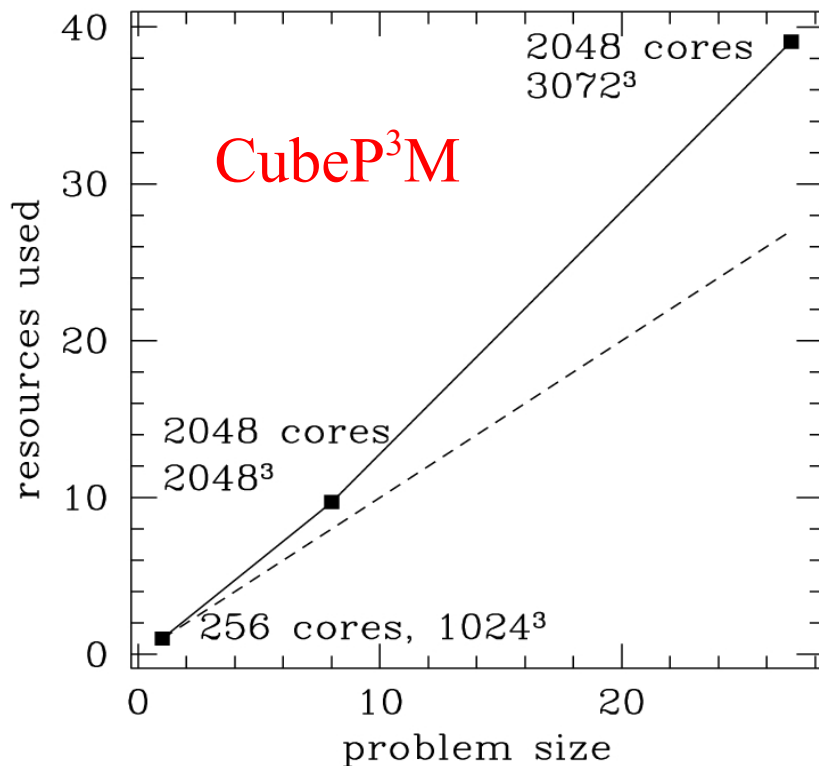
Coupled to hydro

Code Scaling

(Iliev, Mellema, Merz, Shapiro, Pen 2008 in TeraGrid08 proceedings)

Both N-body and radiative transfer codes are massively parallel and scale (weakly) up to thousands of processors.

Full, detailed radiative transfer|: Petascale-size problem!



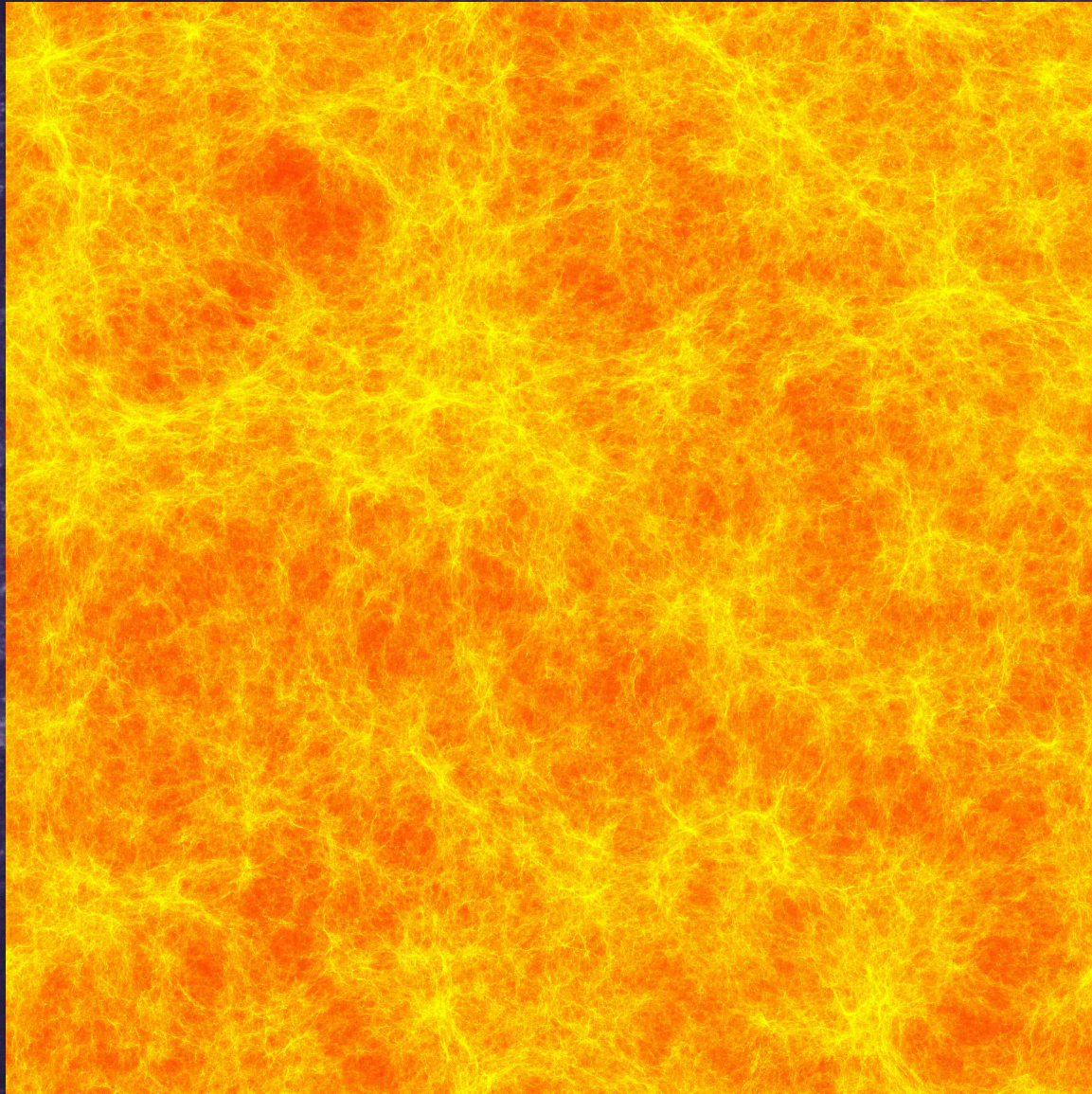
The Formation of Early Cosmic Structures

Iliev, Mellema, Pen, Merz, Shapiro, Alvarez 2006a, MNRAS, 369, 1885, and in progress)

114/h Mpc box @ $z=6$
3072³ particles (29 billion),
6144³ cells, P³M simulation

We have now ran simulations with
1024³, 1500³, 1728³, 2048³ and 3072³
particles in boxes of 37/h-114/h Mpc.
Still larger simulations are possible
on current hardware, with
64-300 billion particles
(6x-30x the Millenium simulation)
165 billion (5488³; on 10,976 cores)
is running; 10¹² (10,000³=trillion)
-particle simulations are now within
reach..

**These sizes allow us to resolve all
halos down to the atomically-cooling
limit ($10^8 M_{\text{solar}}$) in 100-150/h Mpc
boxes - the ultimate goal for
this type of simulations.**



Simulations ran at Texas Advanced
Computing Facility on 432 to 2048 cores.

The Formation of Early Cosmic Structures: The Very Small Scales

(Iliev, et al., work in progress)

11.4/h Mpc box @ $z=8$
3072³ particles (29 billion),
6144³ cells, P³M simulation

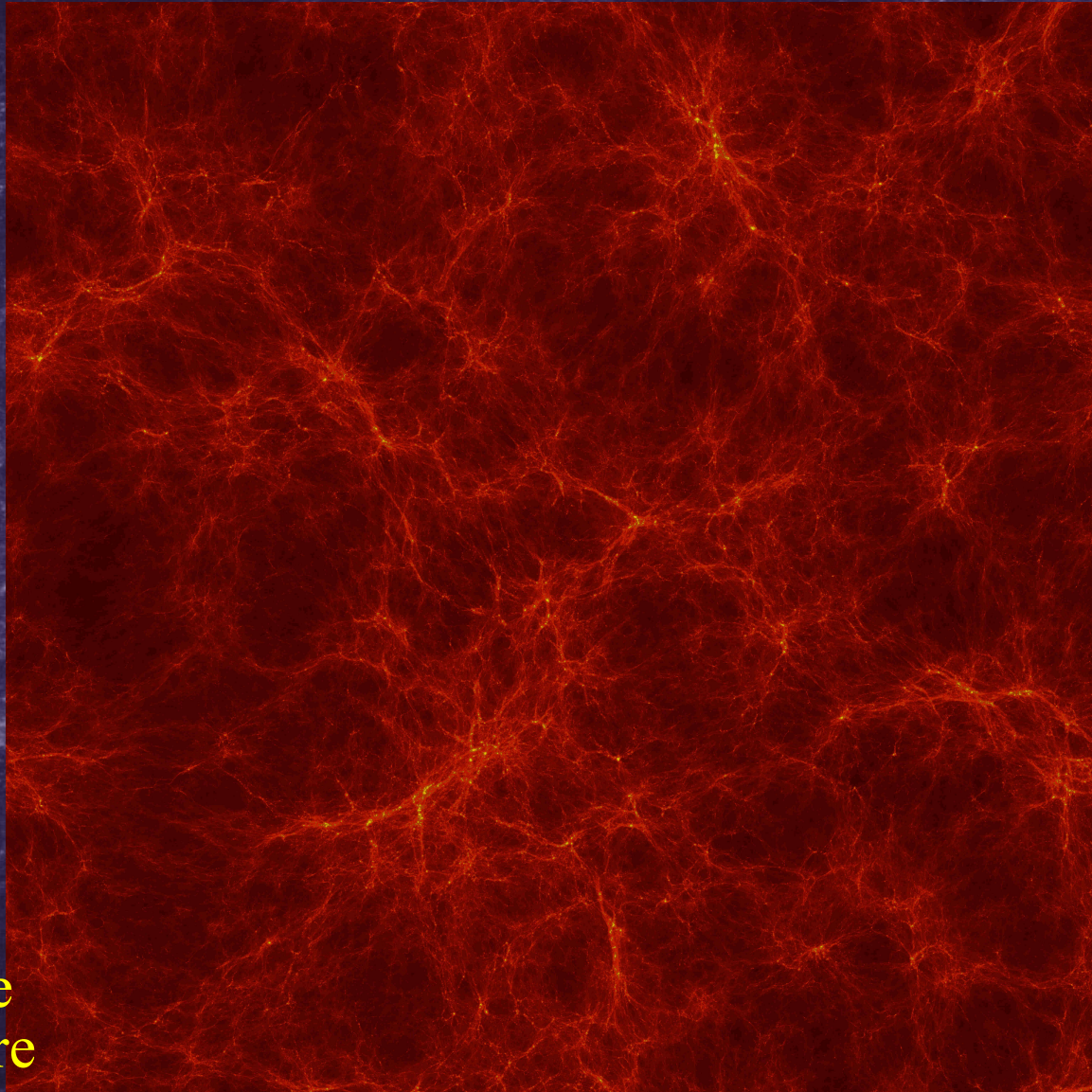
Resolves all halos down to small
minihalos ($10^5 M_{\text{solar}}$).

Structures are highly biased!
Extend to extremely small
scales.

First resolved halos form at
 $z=40$.

>21 million halos at $z=8$.

Very useful for modelling the
effects of small-scale structure
and 21-cm absorption.



Simulation ran at Texas Advanced
Computing Center on 2048-4096 cores.

The Formation of Early Cosmic Structures: The Very Small Scales

(Iliev, et al., work in progress)

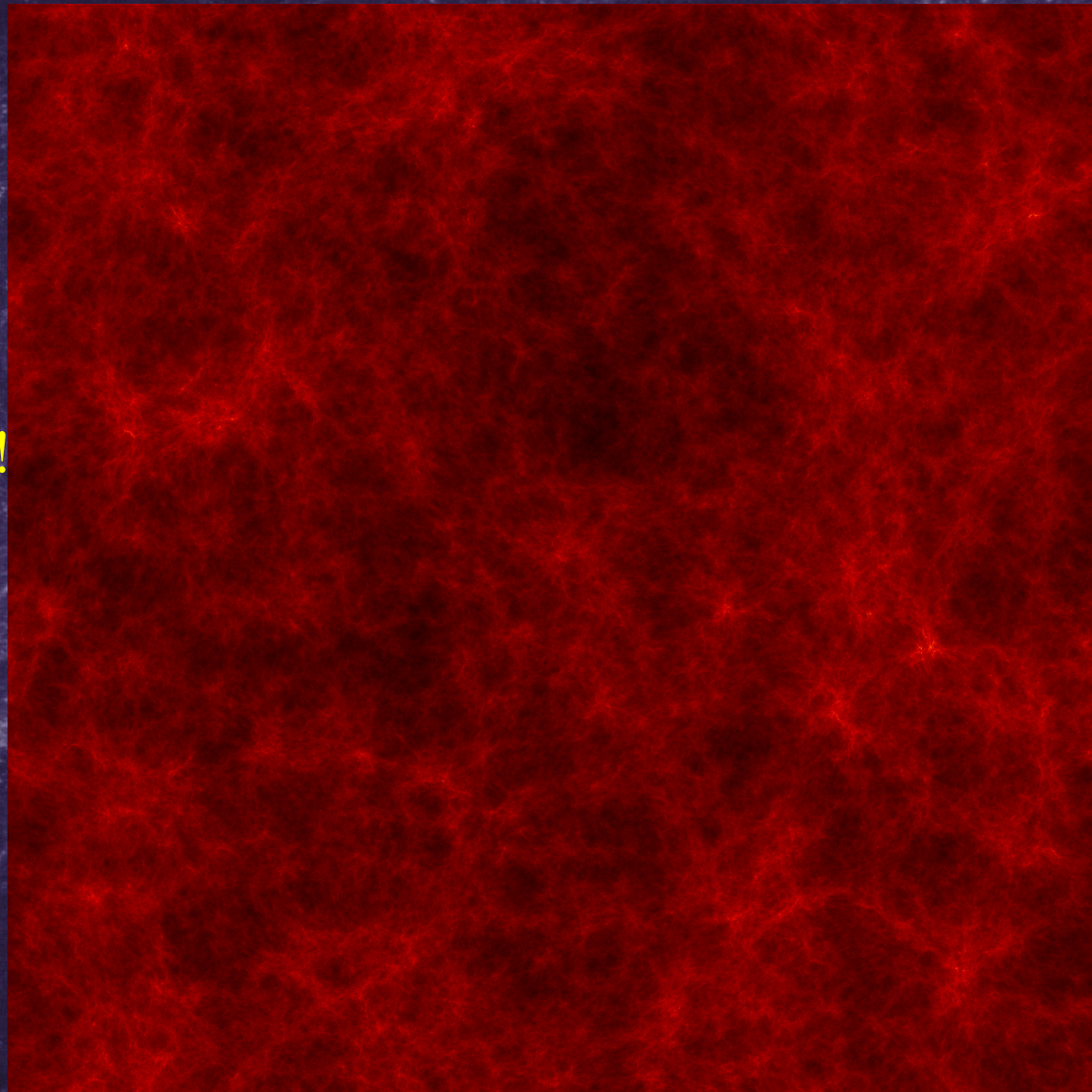
20/h Mpc box @ $z=20$
5488³ particles (165 billion),
10976³ cells, P³M simulation

Resolves all halos down to small
minihalos ($10^5 M_{\text{solar}}$).

Structures are highly biased!
Extend to extremely small
scales (resolution of this
simulation is 182 pc!)

First resolved halos form at
 $z=43$.

>40 million halos at $z=14.7$
(still running).



Simulation ran at Texas Advanced
Computing Center on 21952 cores.

Universe in a Box: Simulating the Observable Universe

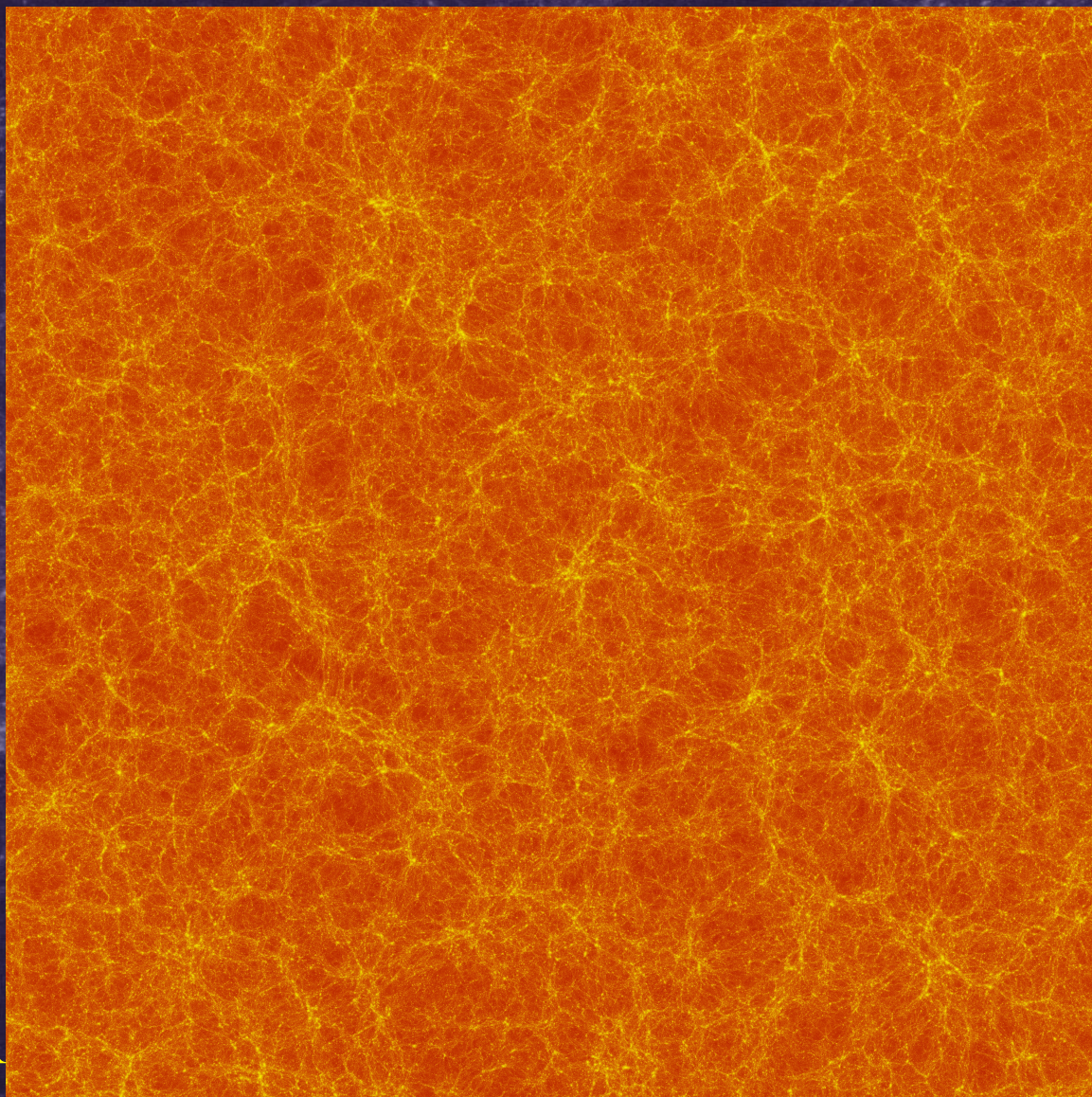
(Desjacques, Seljak & Iliev 2008, and in prep.)

1/h Gpc box @ $z=0.28$
3072³ particles (29 billion),
4096³ cells, P³M simulation
over 40 million halos at low z 's

Series of sims with 64 billion
(4000³) particles (on 4000 cores)
and 3.2 Gpc/h box is in progress

These sizes allow simulating
the whole volume of a large
galaxy survey (multiple Gpc³)
with the appropriate resolution
(i.e. resolving L^* or better) – up
to 1 billion galaxies! Ideal for
LOFAR/SKA HI surveys (BAO,
nonlinear bias, non-gaussianity).

Useful also for modelling LOFAR
foregrounds (5x5 deg FOV)



Simulation ran at Texas Advanced
Computing Facility on 2048 cores.

Simulating the Observable Universe
(Mok & Heav 2008, and in prep.)

the whole volume of a large
galaxy survey (multiple Gpc³)
with the appropriate resolution
(i.e. resolving L* or better) – up
to 1 billion galaxies! Ideal for
LOFAR/SKA HI surveys (BAO,
nonlinear bias, non-gaussianity).

Useful also for modelling LOFAR
foregrounds (5x5 deg FOV)

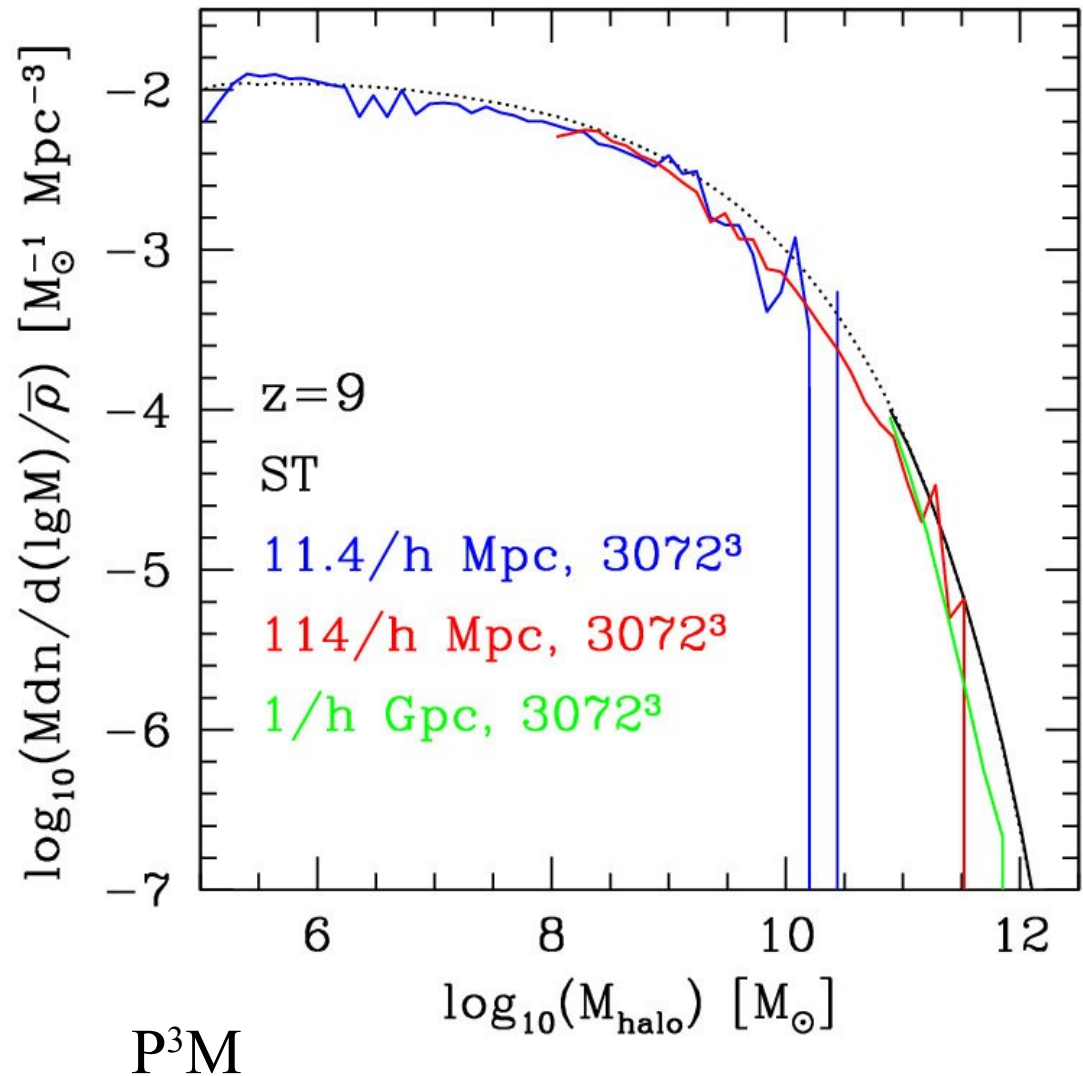
Simulation ran at Texas Advanced
Computing Facility on 2048 cores.

The high-z halo mass function

(work in progress)

Up to ~ 38 (21,21) million halos identified by $z=0$ (6,8) for 1Gpc/h, 114 Mpc/h, 11.4 Mpc/h.

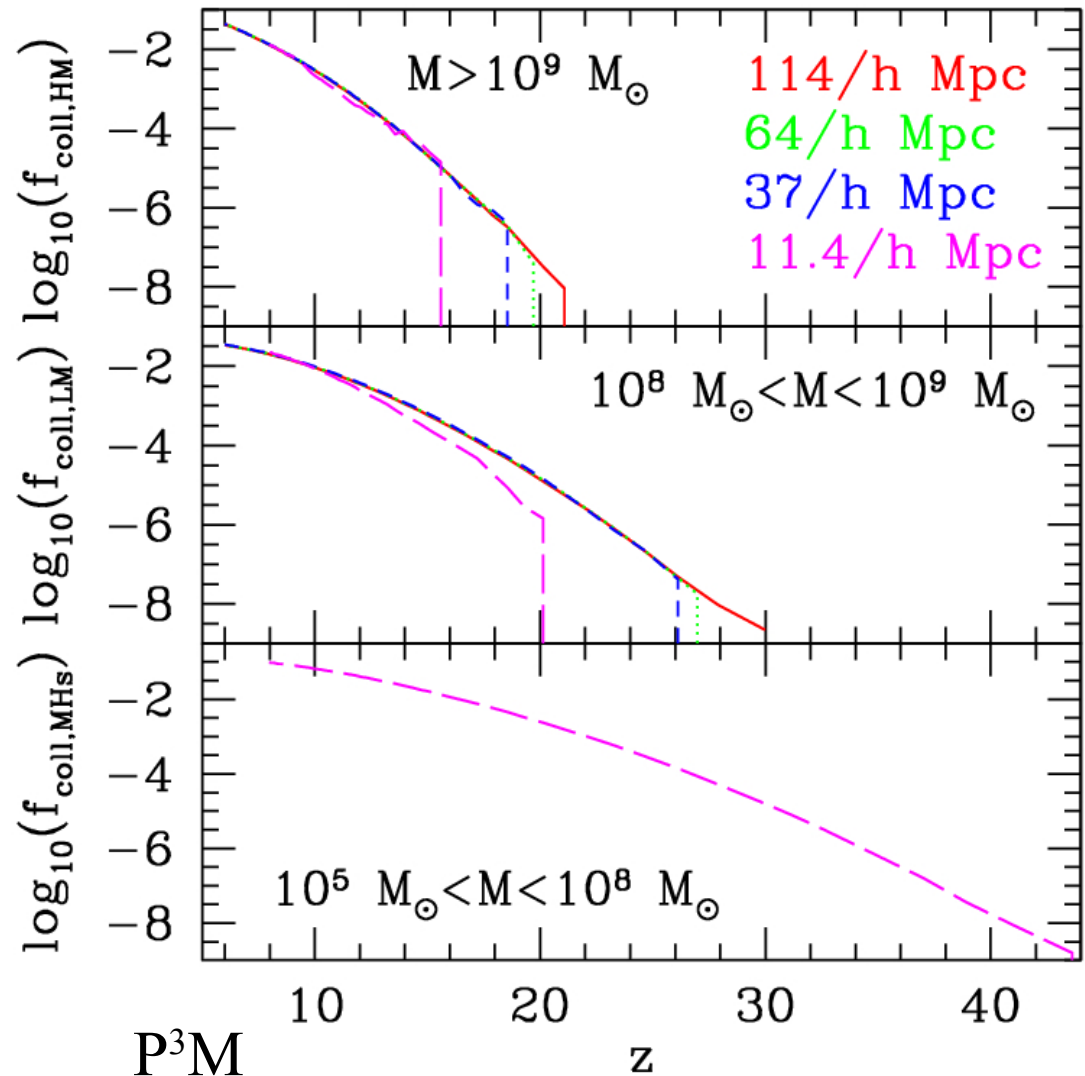
Results show good agreement with each other, but differ from the Sheth-Tormen mass function (black).



The high- z collapsed fractions

(work in progress)

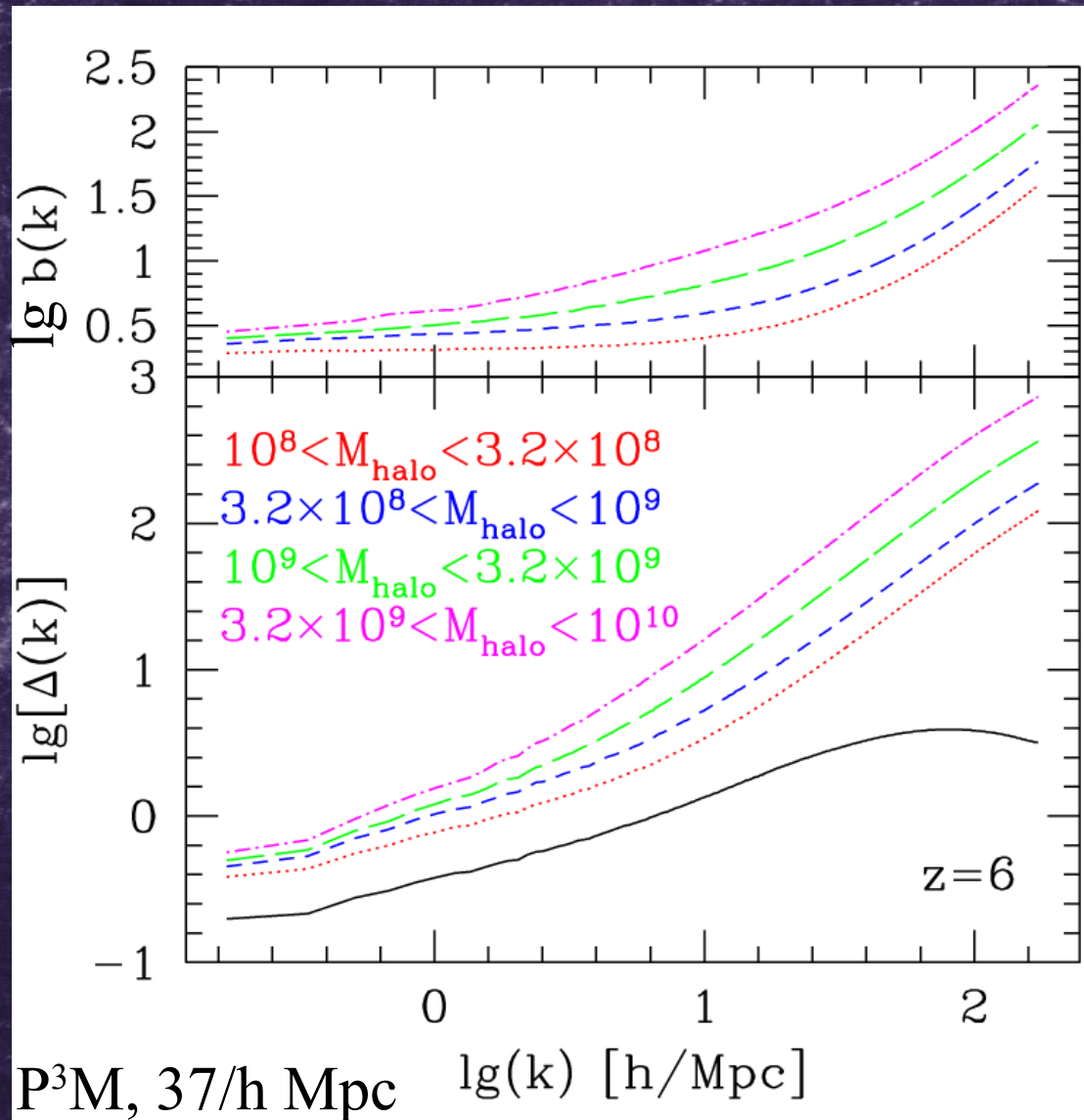
Halo collapsed fractions agree quite well for a range of box sizes from 114 Mpc/h to 11.4 Mpc/h. Deficiency of large halos for the smallest box due to poor statistics.



The high-z halo bias

(work in progress)

- Halos at high- z are strongly biased.
- Bias increases strongly with halo mass and can reach a few hundred in the nonlinear regime.
- Scale at which bias becomes linear varies significantly with halo mass.



Reionization history of sub-regions the highly-patchy nature of reionization

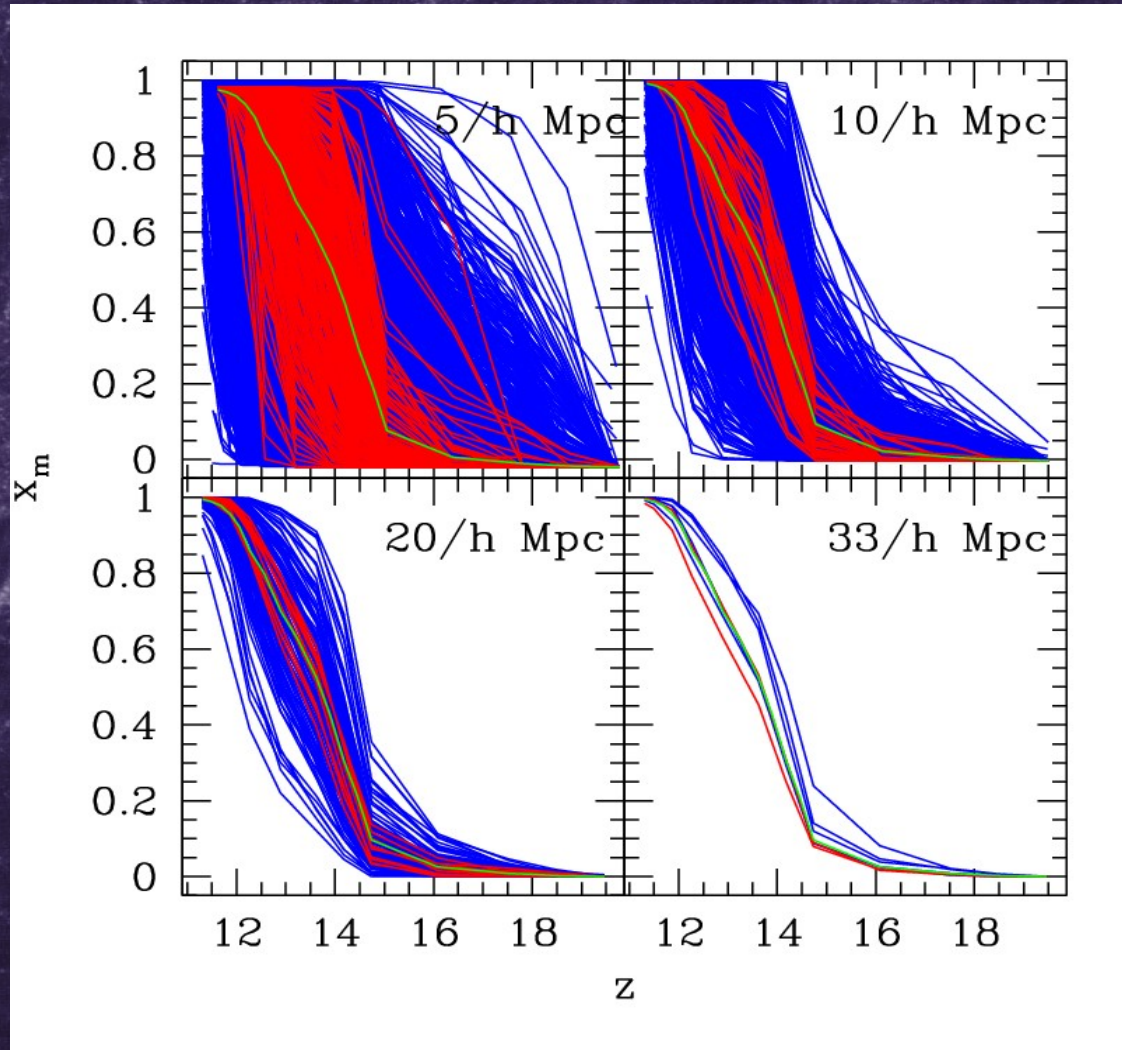
(Iliev, Mellema, Pen, Merz, Shapiro, Alvarez 2006, MNRAS, 369,1625)

green = total mean

red = mean-density
subregions

blue = all sub-regions

For small regions there is huge scatter and overlap epoch cannot be determined well. Only sufficiently large regions (>20 Mpc) describe the mean evolution well (though still larger volumes needed for e.g. HII regions size distribution).



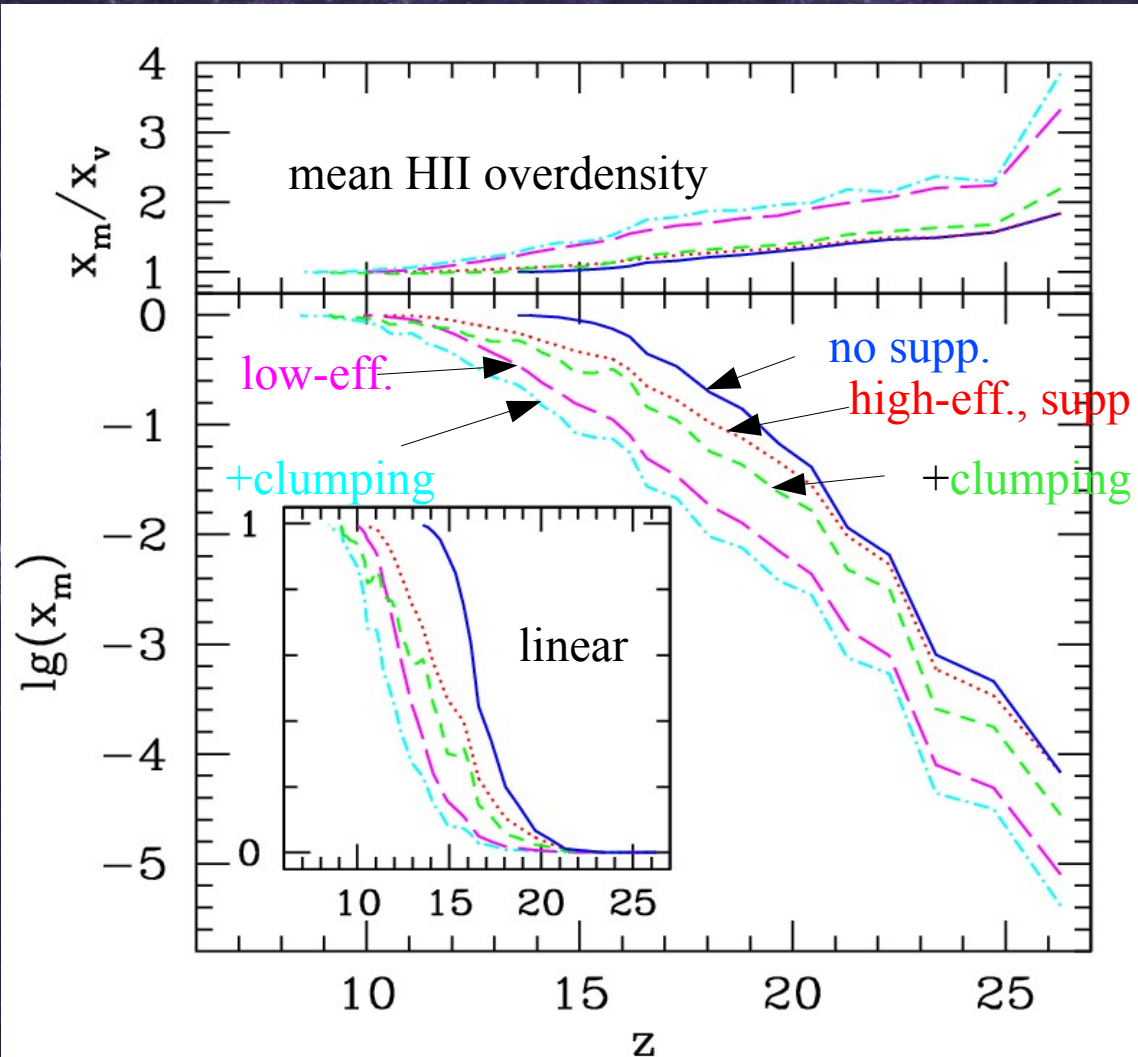
Self-Regulated Reionization

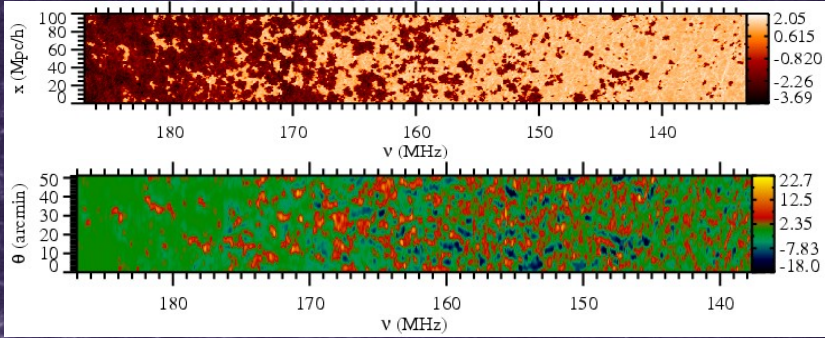
(Iliev, Mellema, Shapiro and Pen 2007a, MNRAS, 376, 534)

Lower large-source efficiencies, Jeans-mass filtering of small sources and time-increasing sub-grid gas clumping all extend reionization and delay overlap.

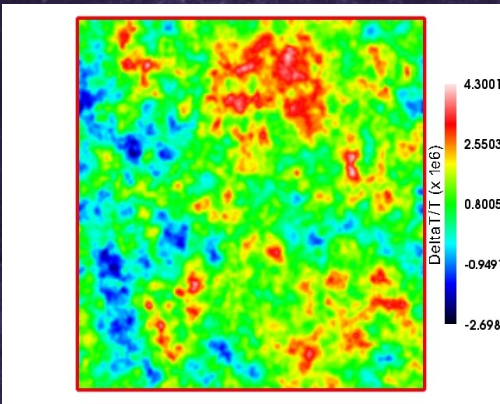
More/less efficient low-mass sources result in more/less suppression of same sources =>

Reionization is **self-regulated**.

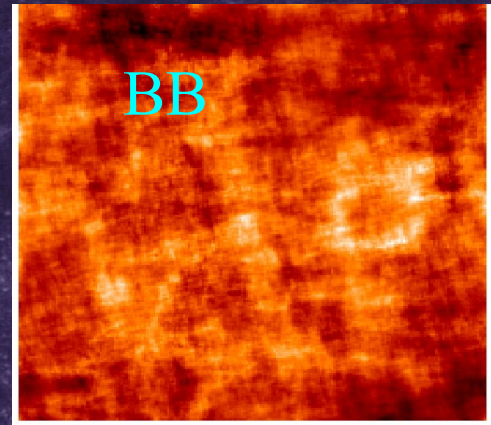




redshifted 21-cm



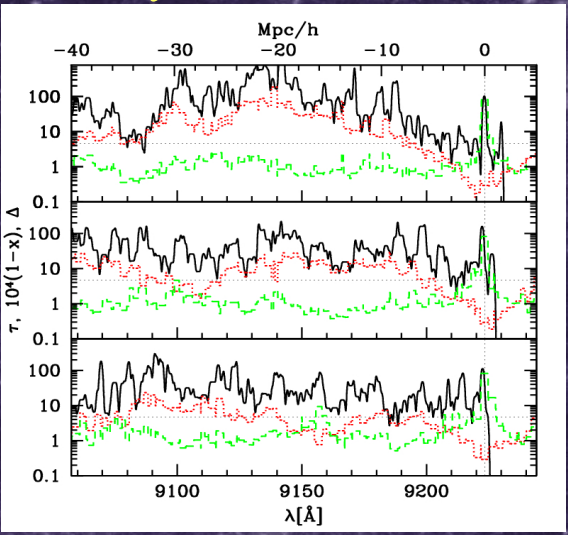
kinetic Sunyaev-Zeldovich effect (kSZ)



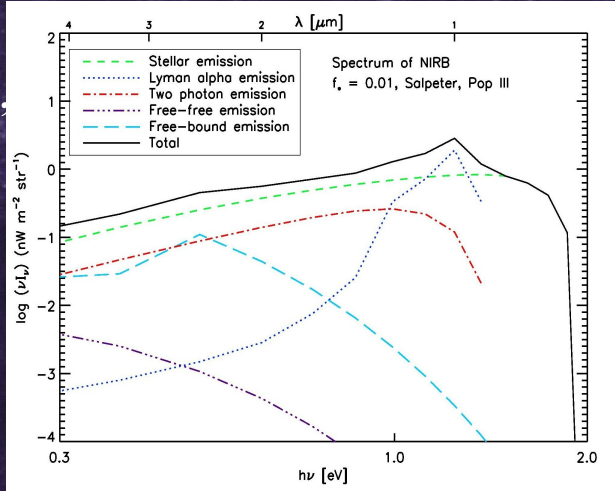
CMB polarization

Observing the Reionization Epoch

Ly- α sources

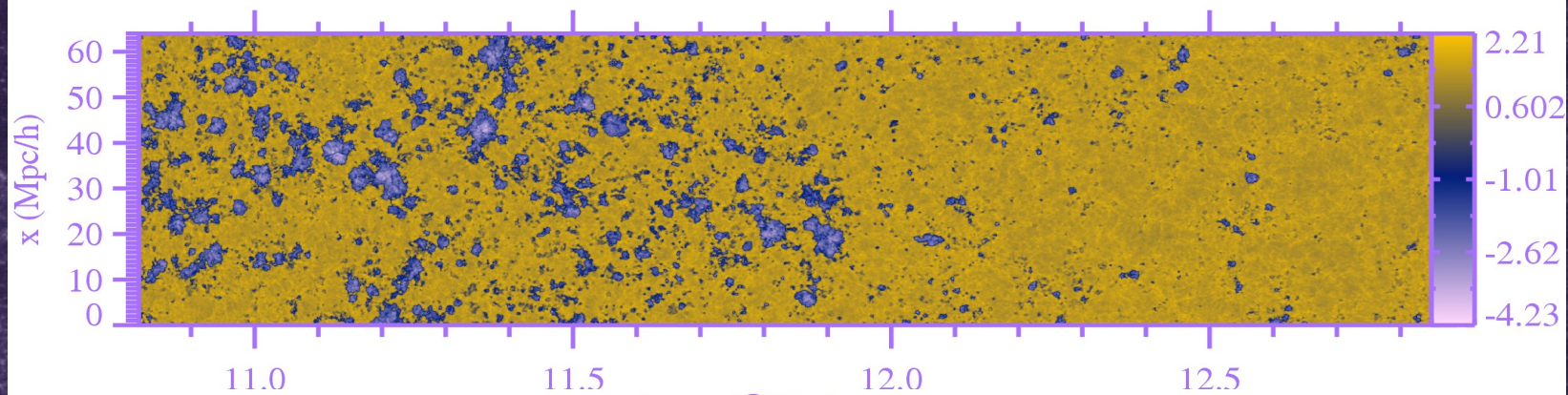


NIR fluctuations



Iliev et al. 2006a, MNRAS; 2007(a,b,c,d), 2008 MNRAS, ApJ, Mellema et al. 2006, MNRAS; Dore et al., 2006, Phys. Rev. D; Holder, Iliev & Mellema 2006 ApJ, Fernandez et al. 2009, Tilvi et al. 2009, submitted

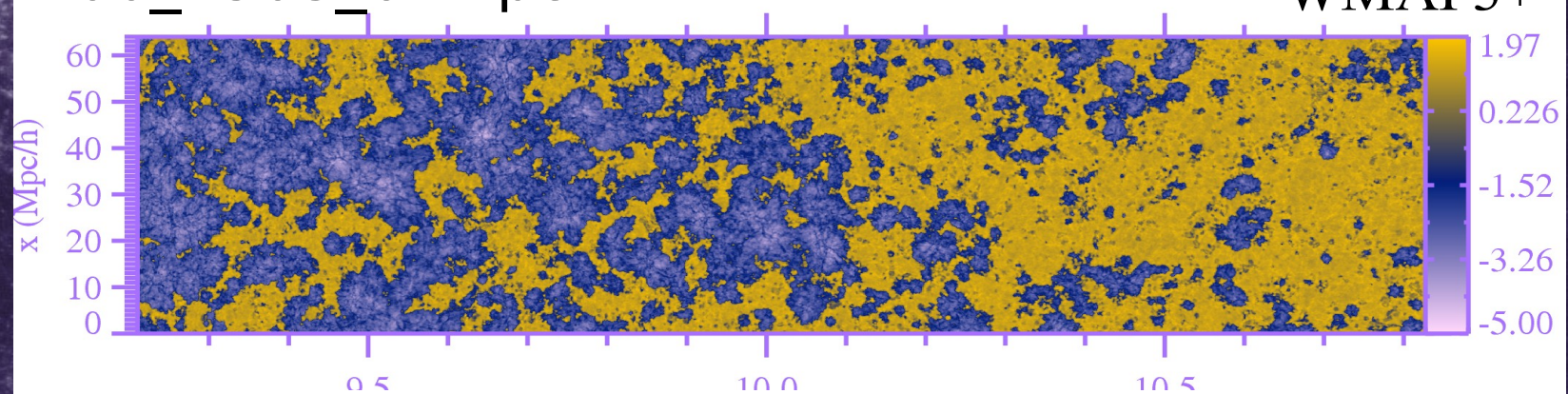
$\log_{10}(\delta T)$ (mK)



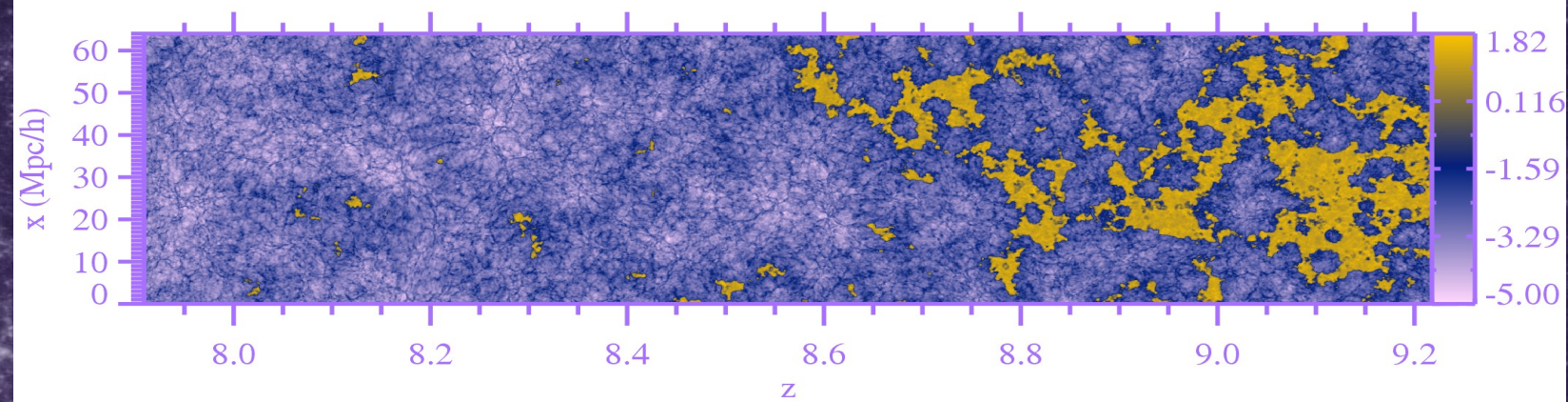
f100_250S_64Mpc

$\log_{10}(\delta T)$ (mK)

WMAP3+



$\log_{10}(\delta T)$ (mK)



Reionization in action as seen at 21-cm: Flying through the Image Cube

21-cm view of EOR

LOS spectra: redshift space distortions

(Mellema, Iliev, Pen, Shapiro MNRAS, 2006)

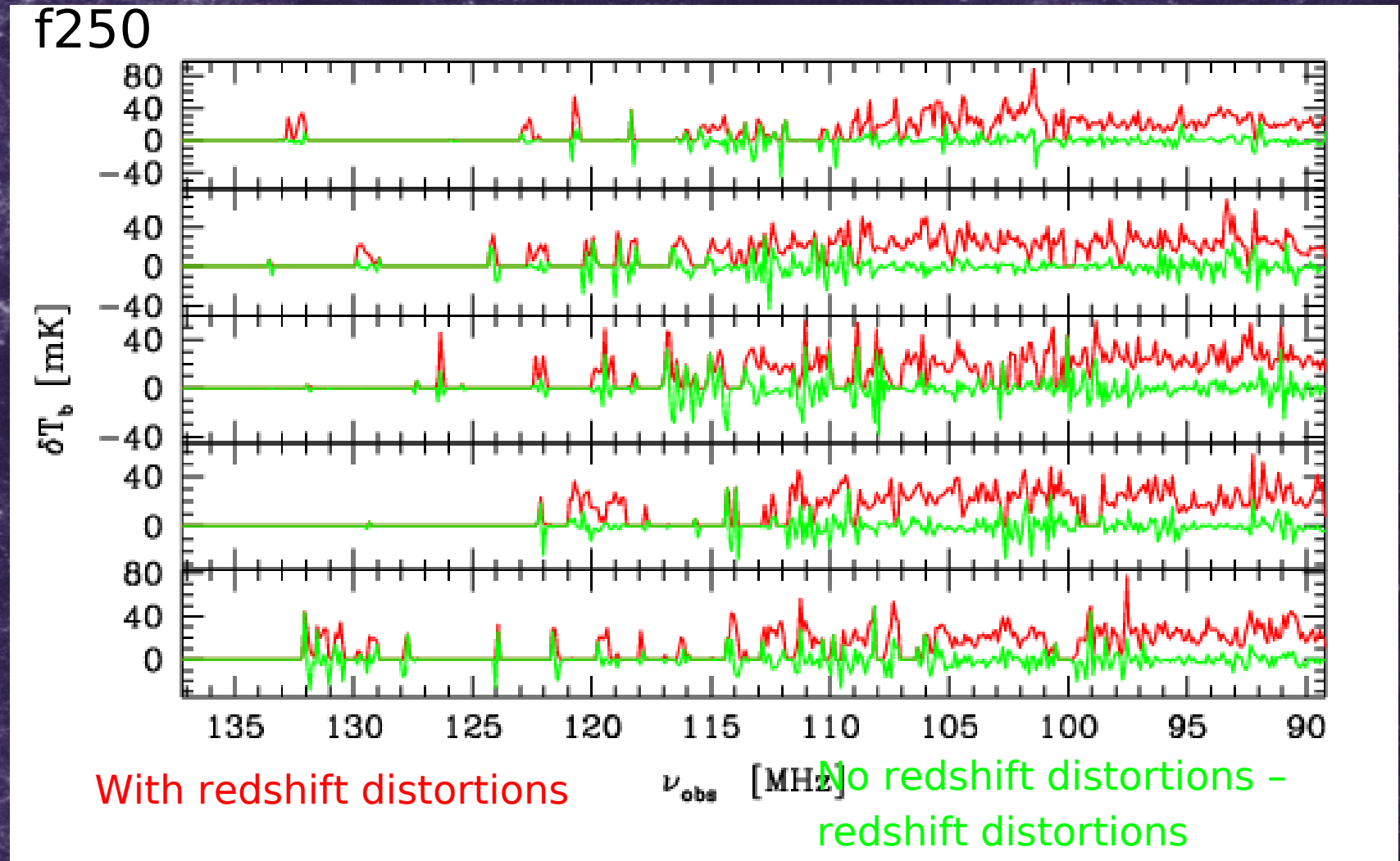


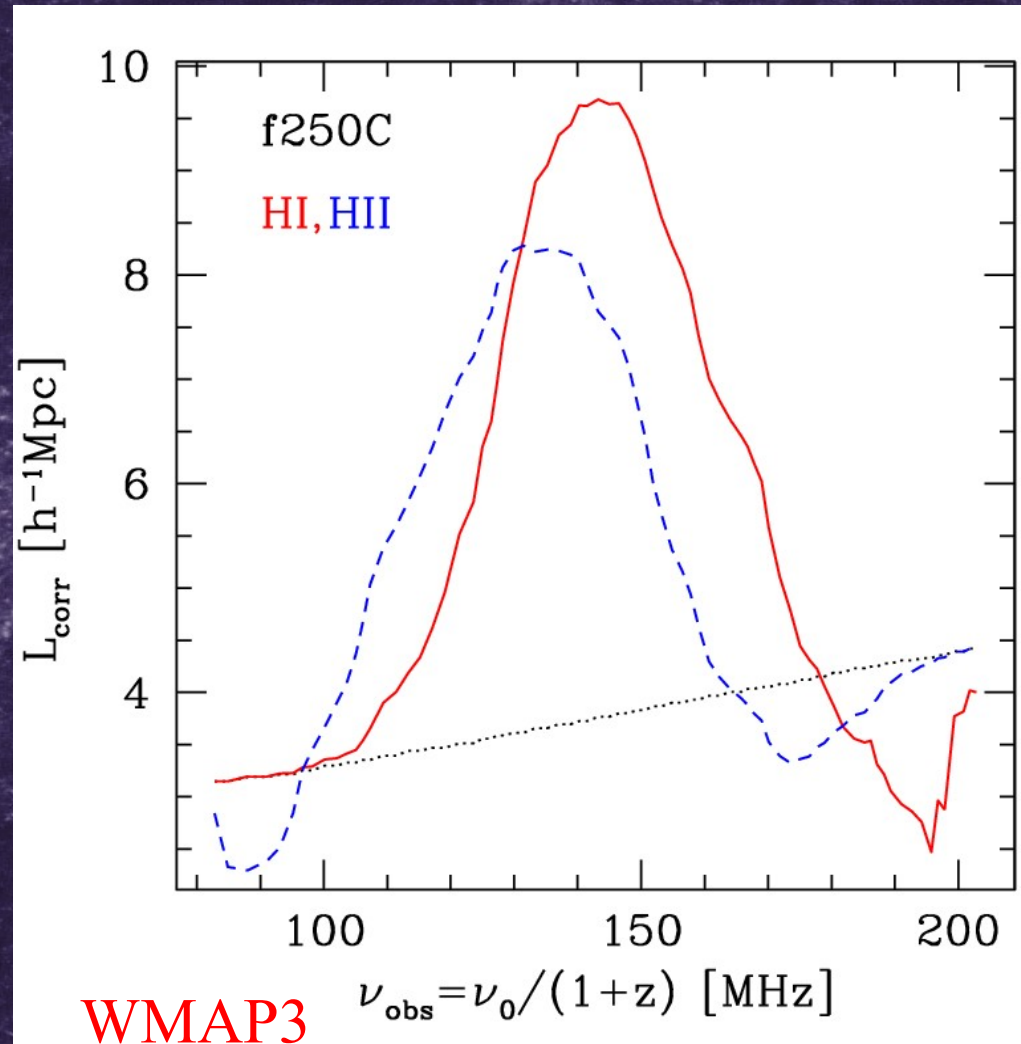
Image correlations

(Iliev, Mellema, Pen, Shapiro, arXiv/0712.1356, PoS)

The correlation lengths between images (freq. slices) show strong evolution, mirroring the characteristic patch size evolution.

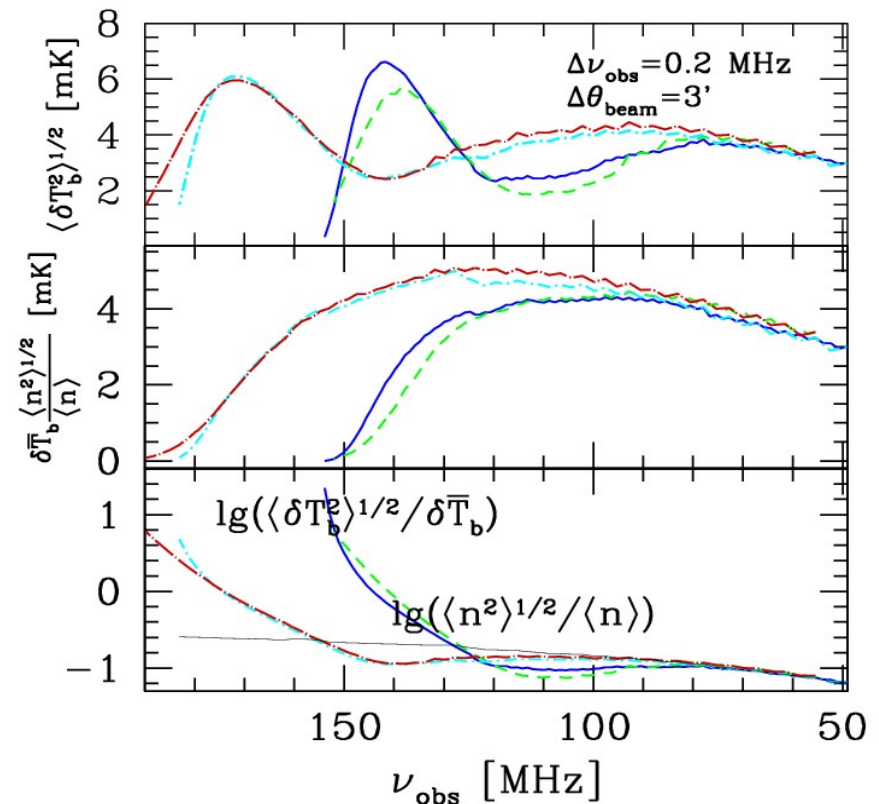
Ionized bubble correlations peak earlier than the ones for the neutral patches.

Useful check on the observations – if the EOR signal is real.

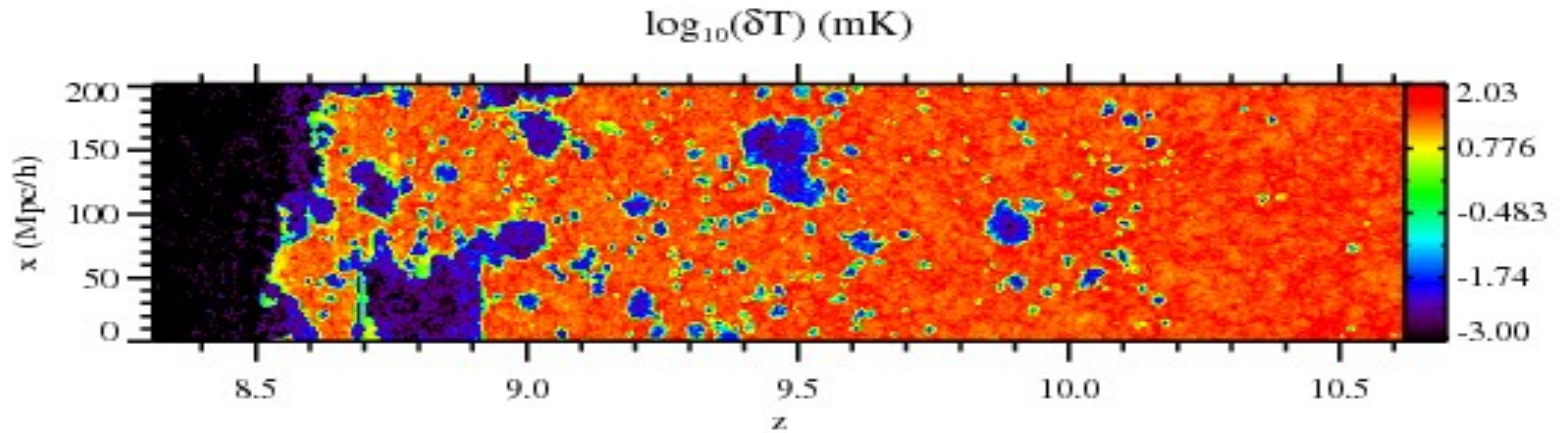


21-cm rms fluctuations: extended vs. early reionization

- Significant boost of fluctuations due to patchiness.
- Similar peak levels, 6-7 mK at LOFAR-like resolution, but at very different frequencies - ~ 140 vs. ~ 170 MHz.
- Small box supresses fluctuations noticeably for early reionization, but not for extended one.

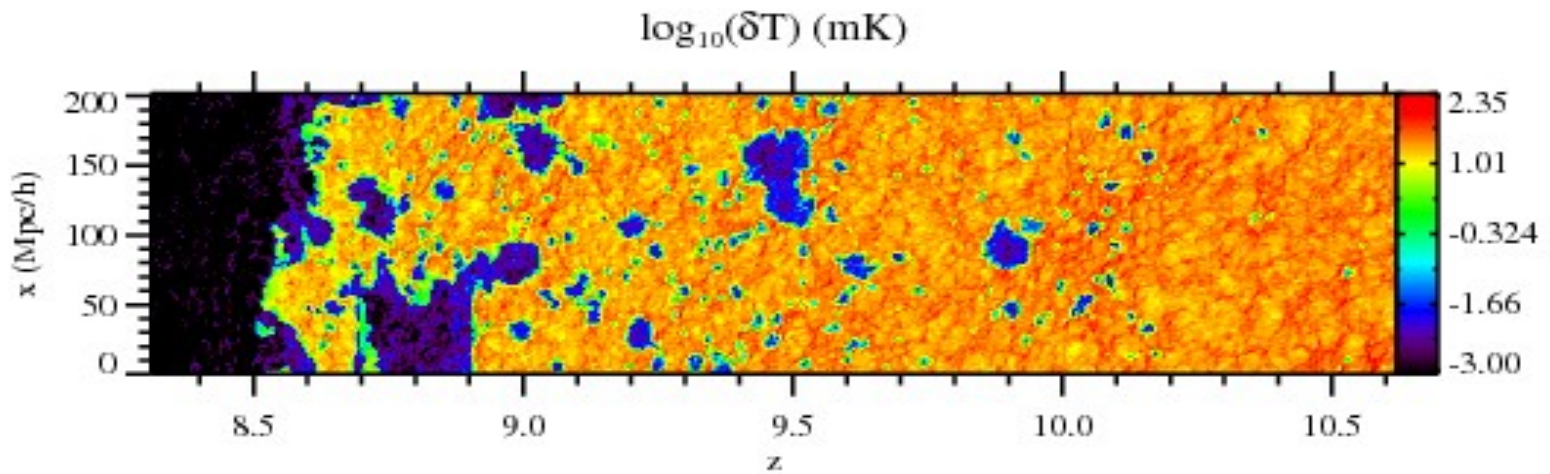


Evolution Slices at 21-cm line: redshift-space distortions and Kaiser effect



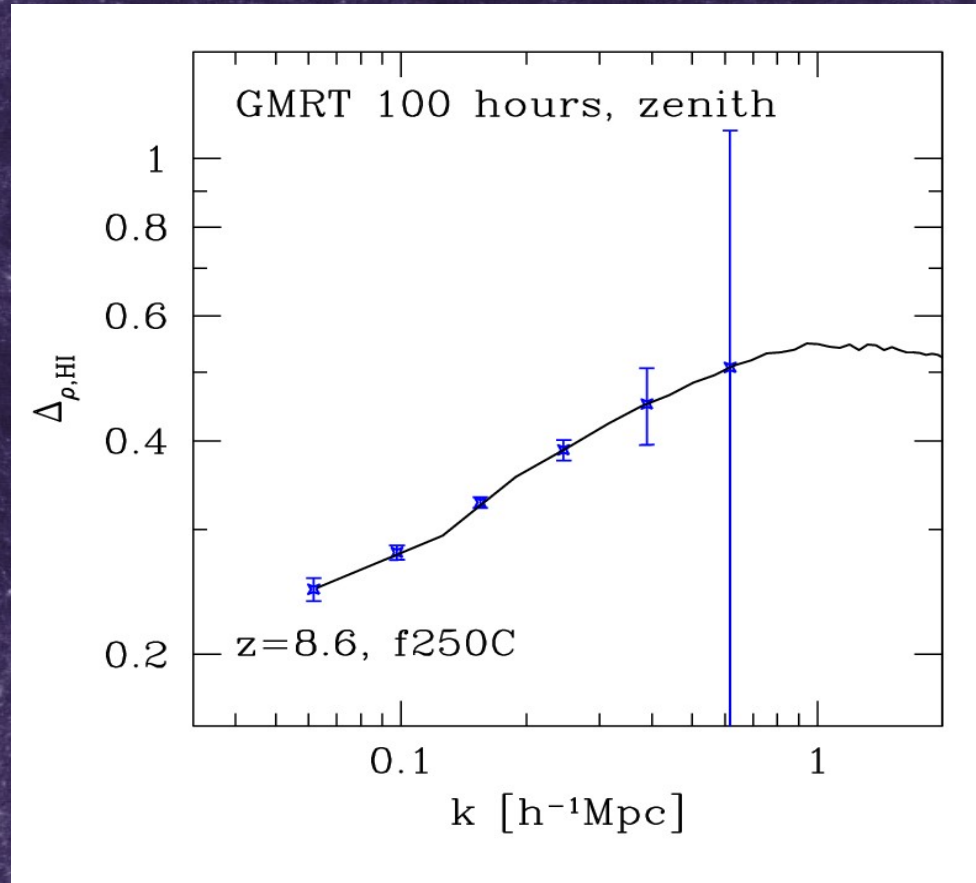
f250C

WMAP3



Detectability of 21-cm

(Iliev, Mellema, Pen, Bond, Shapiro, 2007)

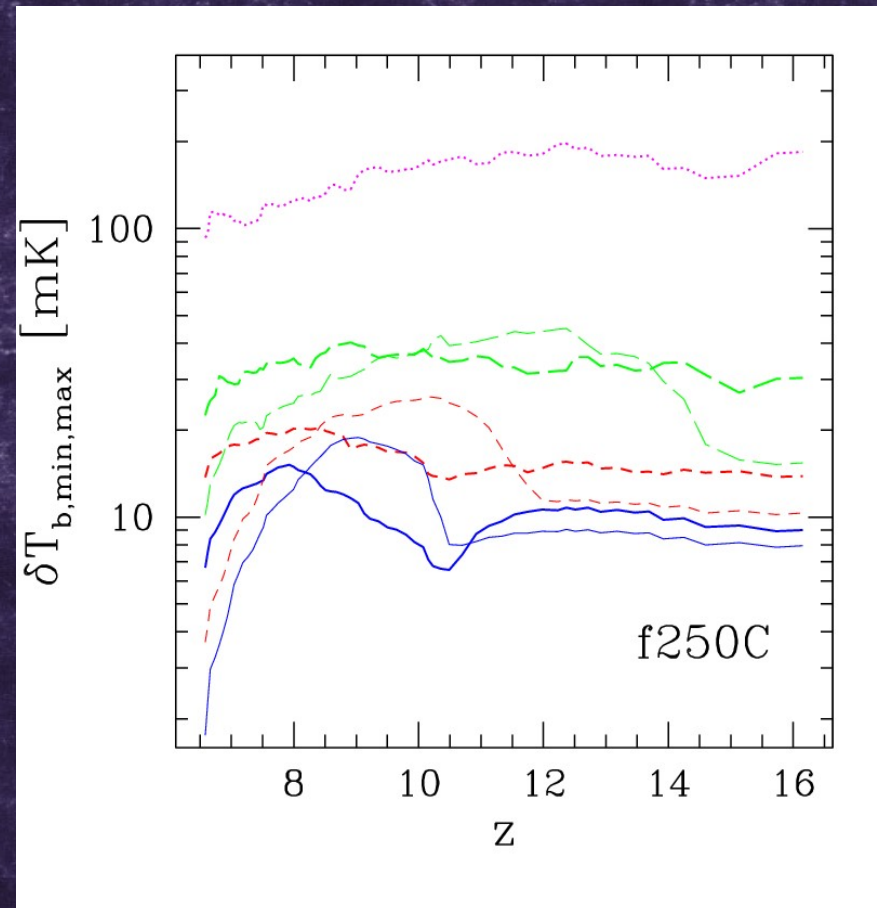
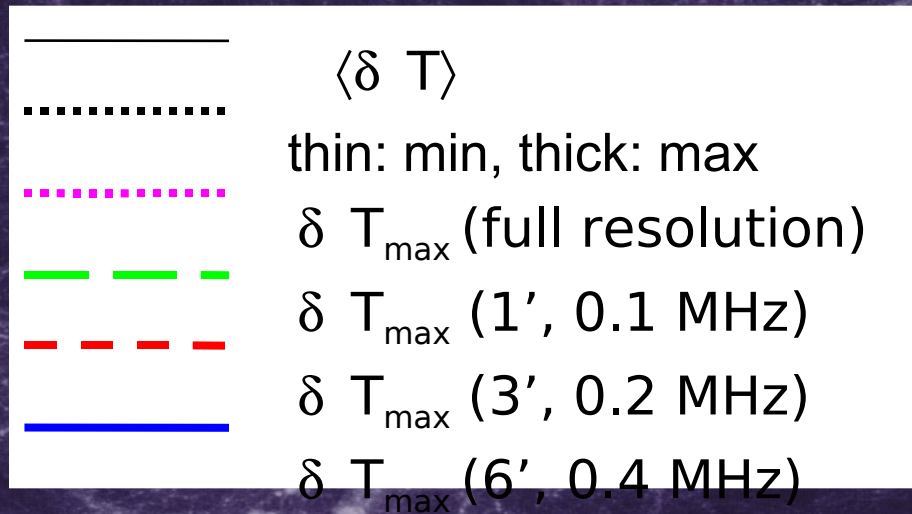


- 3D power spectra of the EoR 21-cm signal (neutral density) vs. noise level of GMRT. Foregrounds will increase error bars at large scales (small k's).

Beyond Gaussian statistics

(Mellema, Iliev, et al. 2006)

- What is the **brightest point** in our volume at a given redshift?

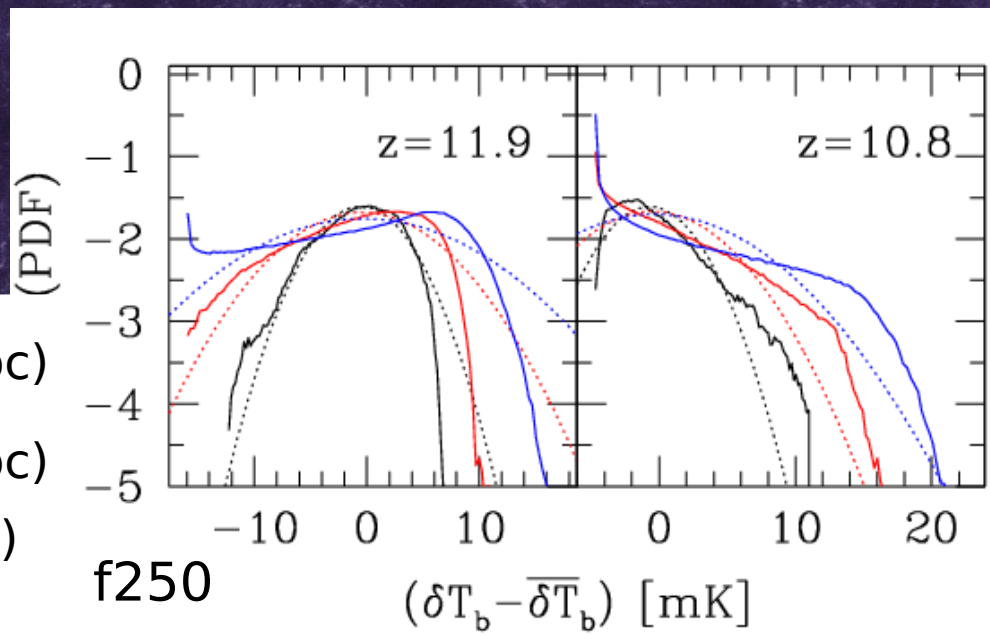


Probability Distribution Functions

(Mellema, Iliev, et al. 2006; Iliev et al. 2008a)

Distribution of δT is highly non-Gaussian, especially at late times.

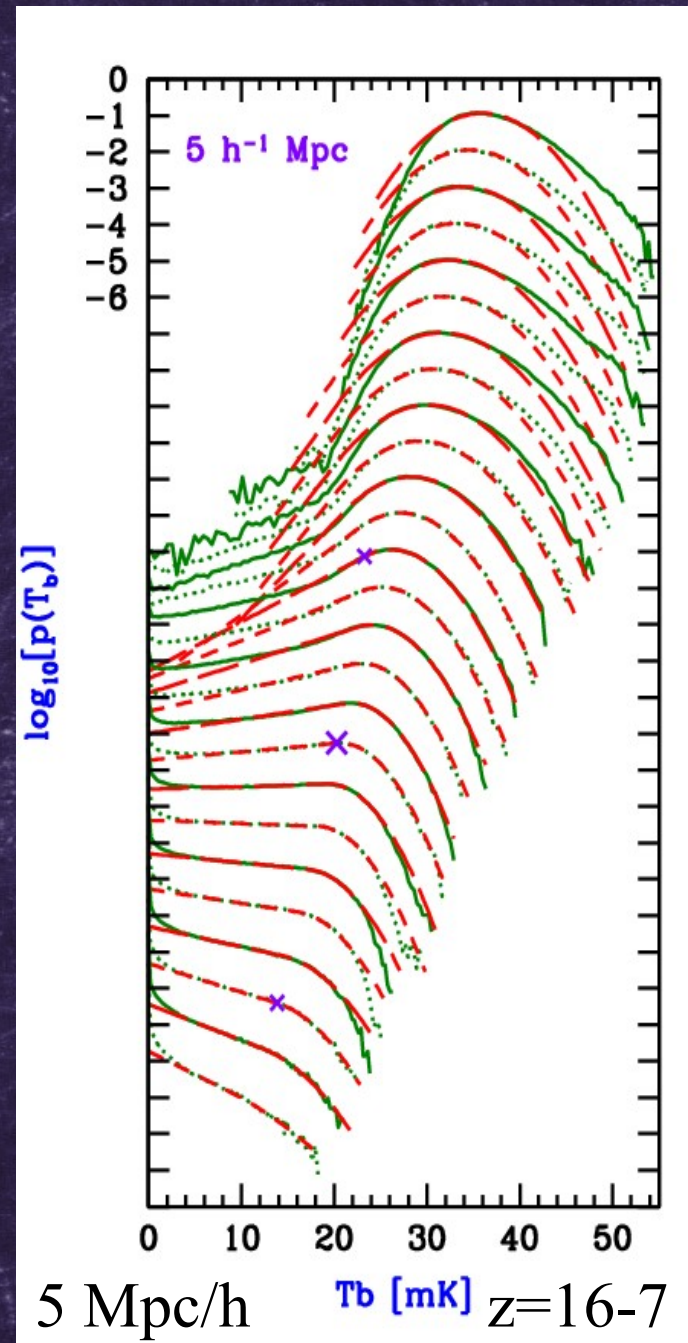
- Gaussian PDF (20/h Mpc)
- Gaussian PDF (10/h Mpc)
- Gaussian PDF (5/h Mpc)
- PDF (20 Mpc/h)
- PDF (10 Mpc/h)
- PDF (5 Mpc/h)



Measuring EoR History using 21-cm PDF

(Ichikawa, Barkana, Iliev, Mellema,
Shapiro, submitted, arXiv/0907.2932)

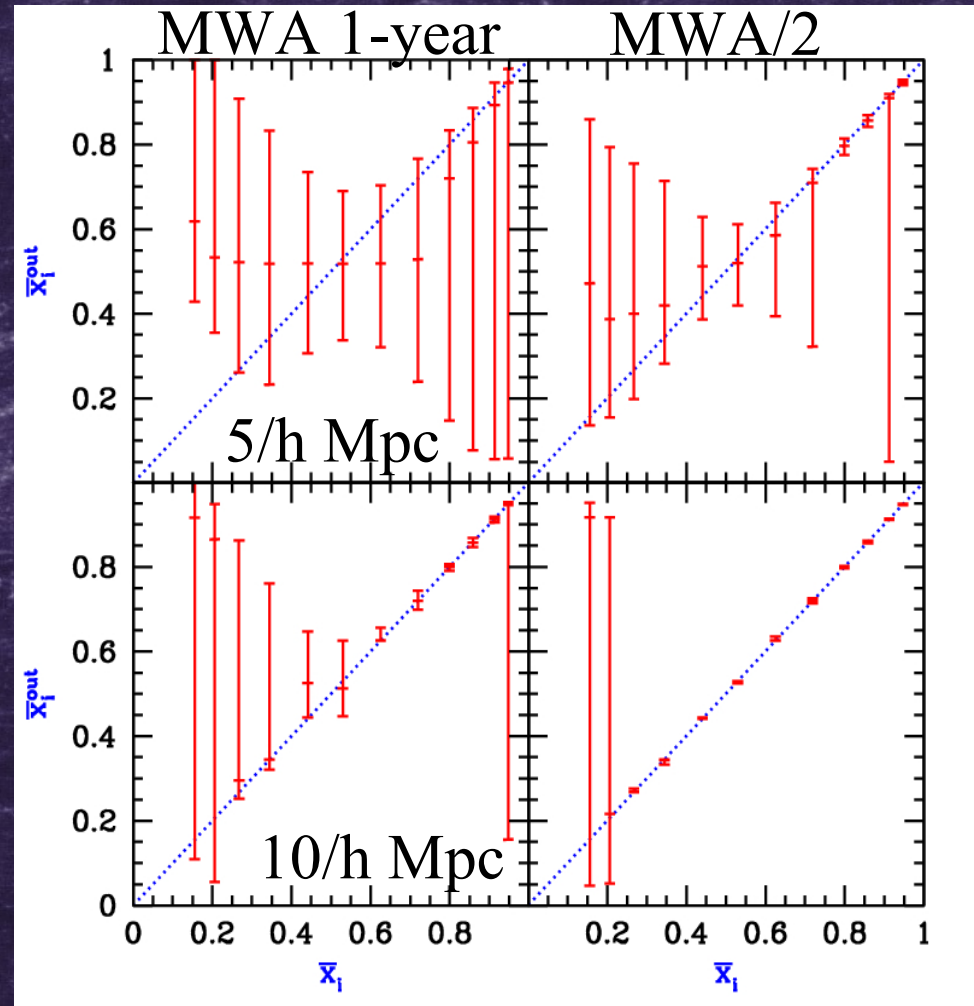
- PDFs are highly non-Gaussian.
- Intermediate PDFs ($x=0.16-95$) are well-fit by exp+Gaussian with 4 free parameters.



Measuring EoR History using 21-cm PDF

(Ichikawa, Barkana, Iliev, Mellema, Shapiro, submitted, arXiv/0907.2932)

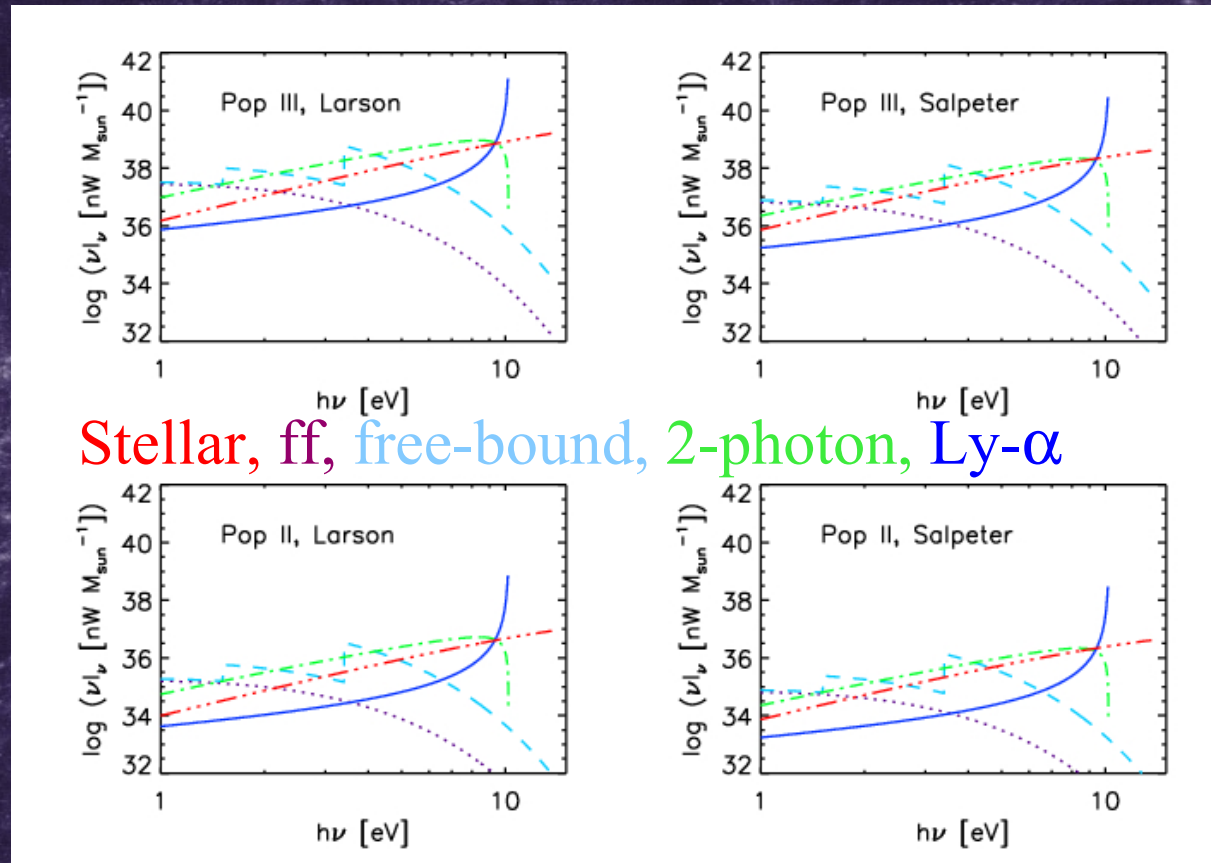
- PDF fits could be used to reconstruct the reionization history:
- E.g. assume PDFs vary with x as in simulations (1-parameter model).
- We generate N_p data points (pixels) with Gaussian noise per pixel.
- Resulting Monte-Carlo generated 'observed' PDF is compared to the model with C-statistics to find the best-fit (see paper for details).



Cosmic Infrared Background Fluctuations

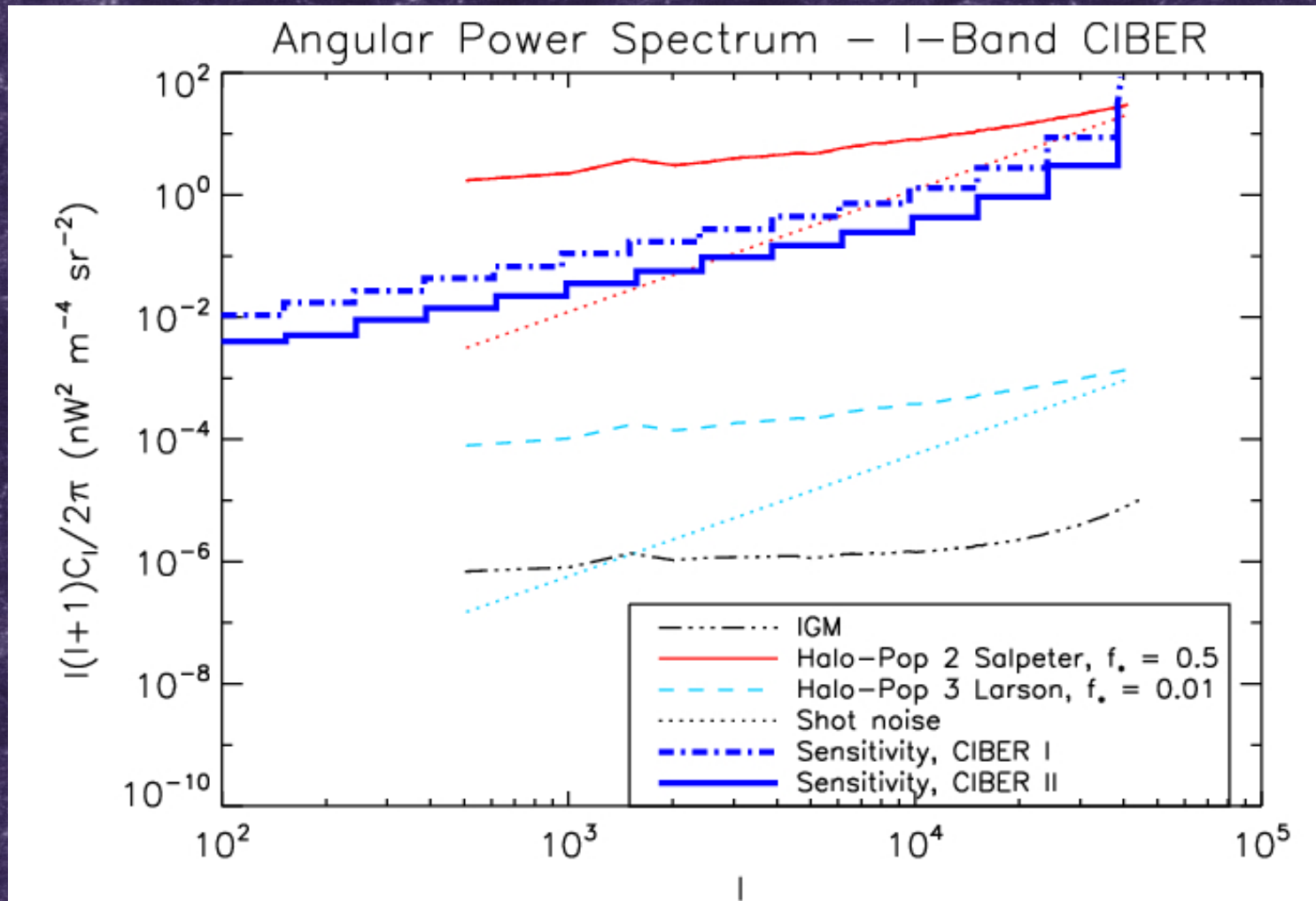
(Fernandez, Komatsu, Iliev & Shapiro, submitted, arXiv/0906.4552)

- N-body+RT data is combined with analytical model for luminosity of early structures (halos+IGM) under different assumptions for the stellar IMF, SF efficiency and escape fractions.



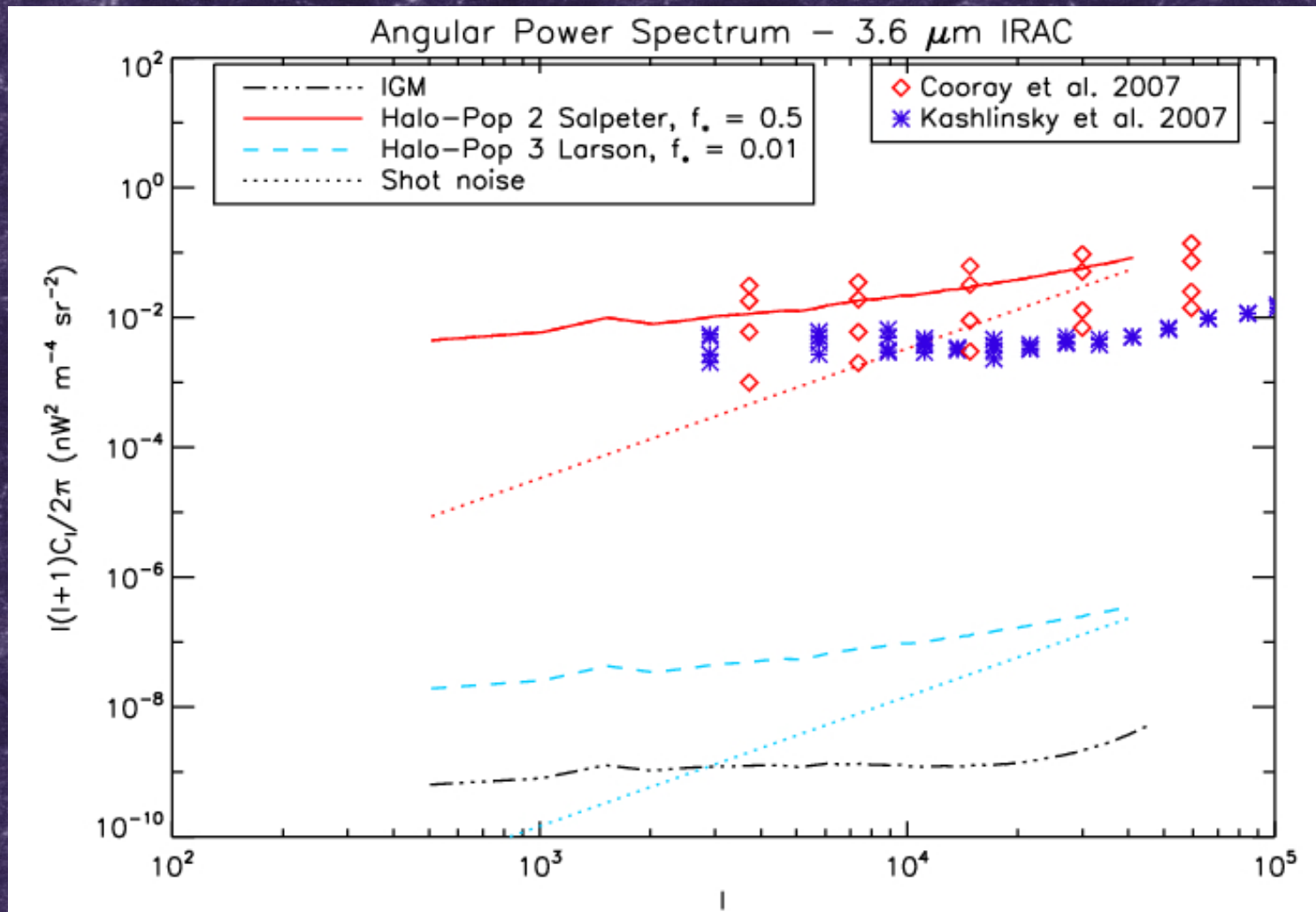
Cosmic Infrared Background Fluctuations: Observability

(Fernandez, Komatsu, Iliev & Shapiro, submitted, arXiv/0906.4552)



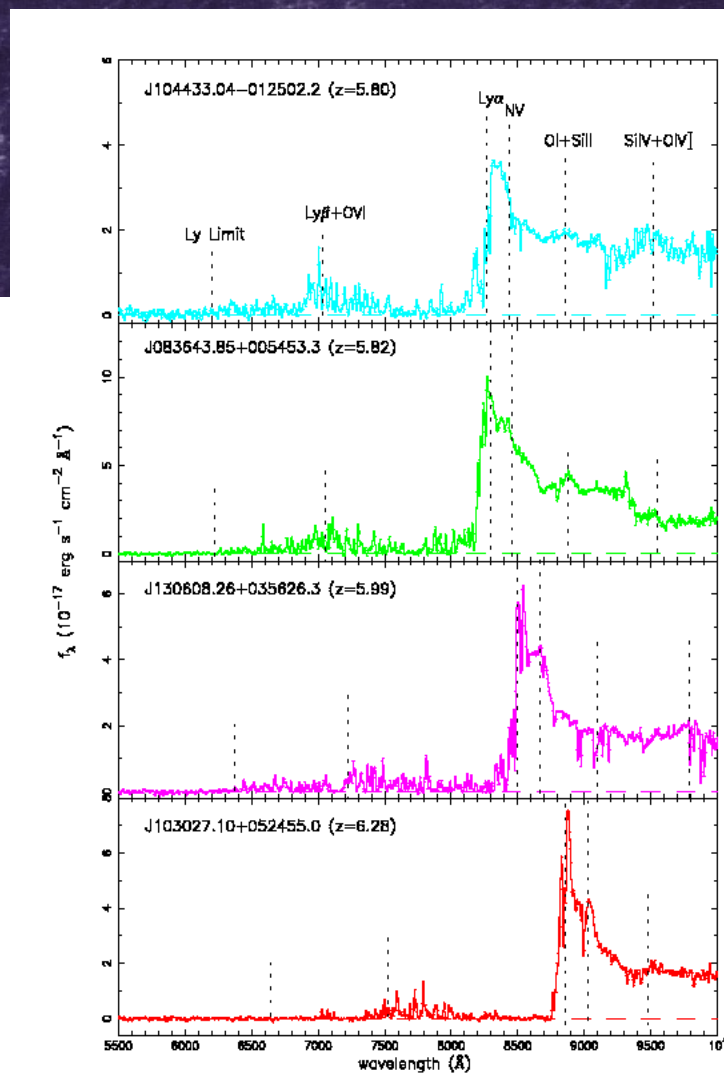
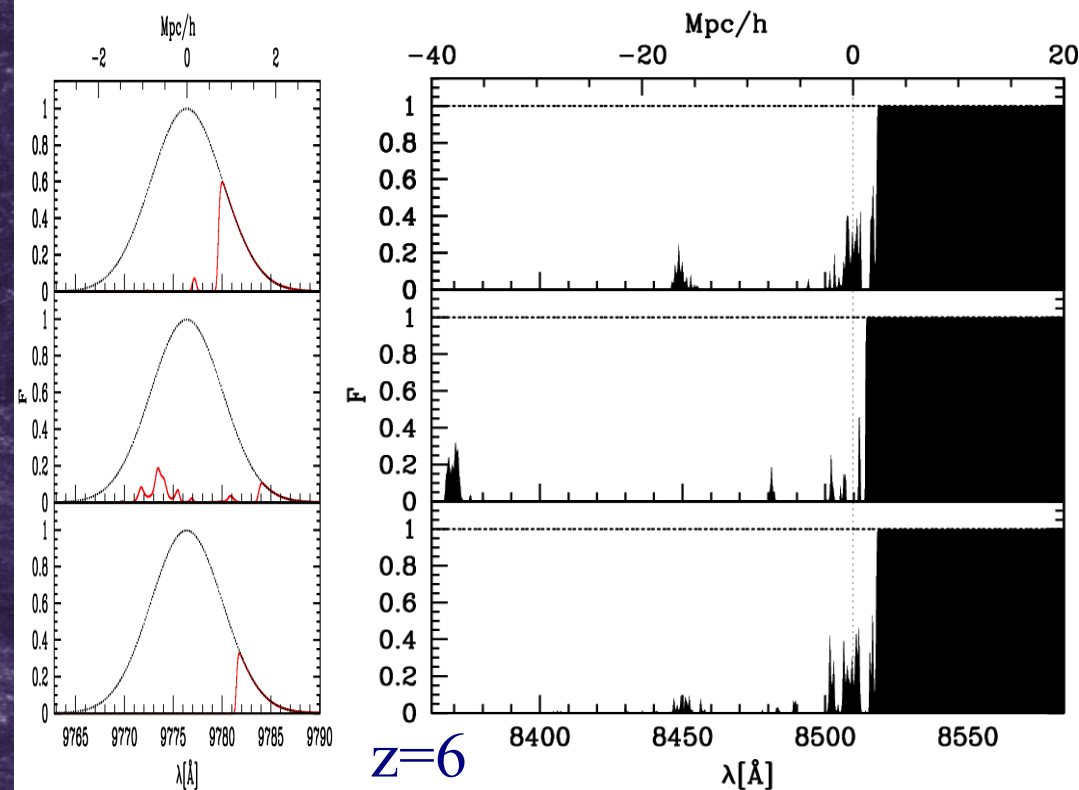
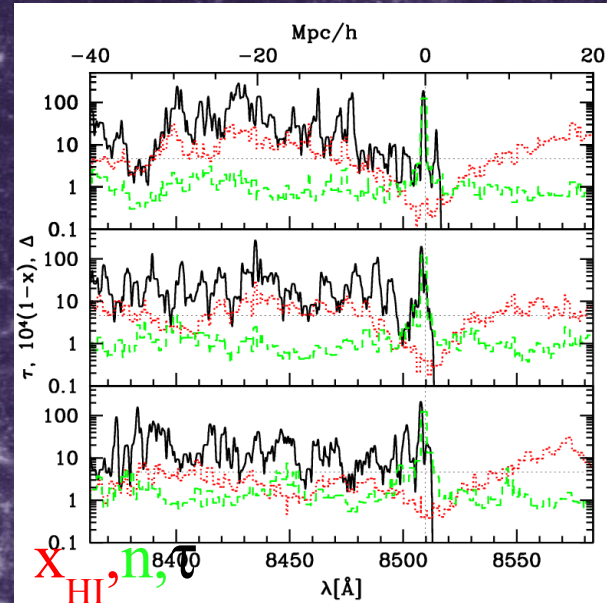
Cosmic Infrared Background Fluctuations: Observability

(Fernandez, Komatsu, Iliev & Shapiro, submitted, arXiv/0906.4552)



Luminous sources at the end of reionization: Ly- α spectra

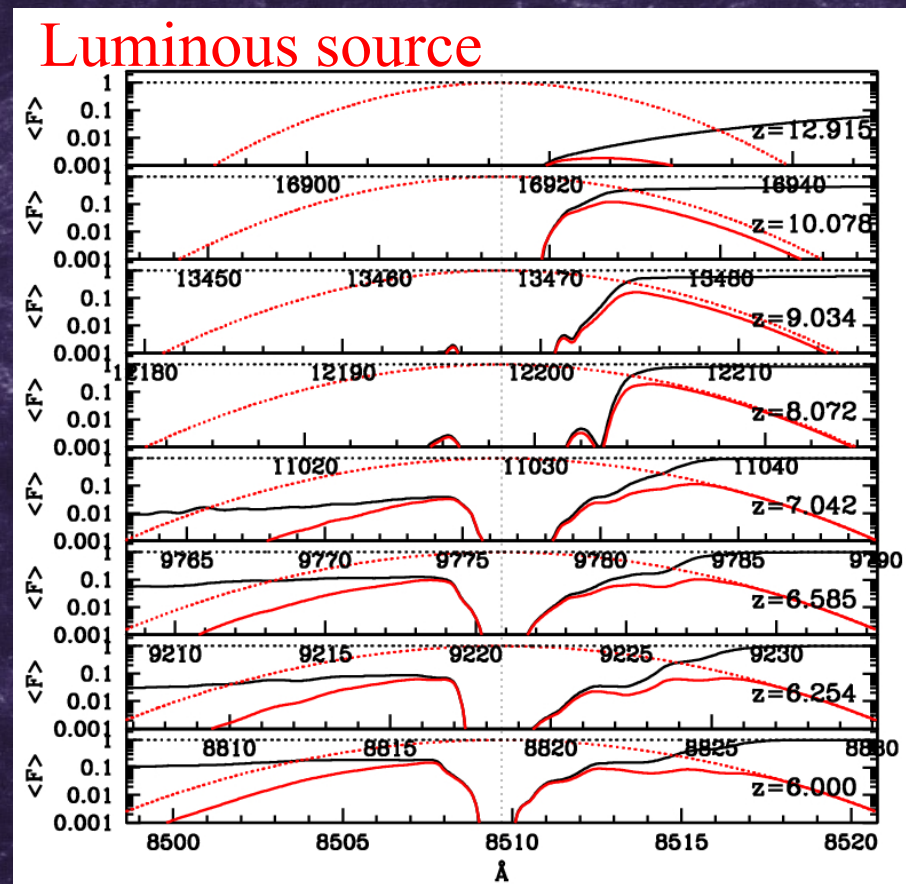
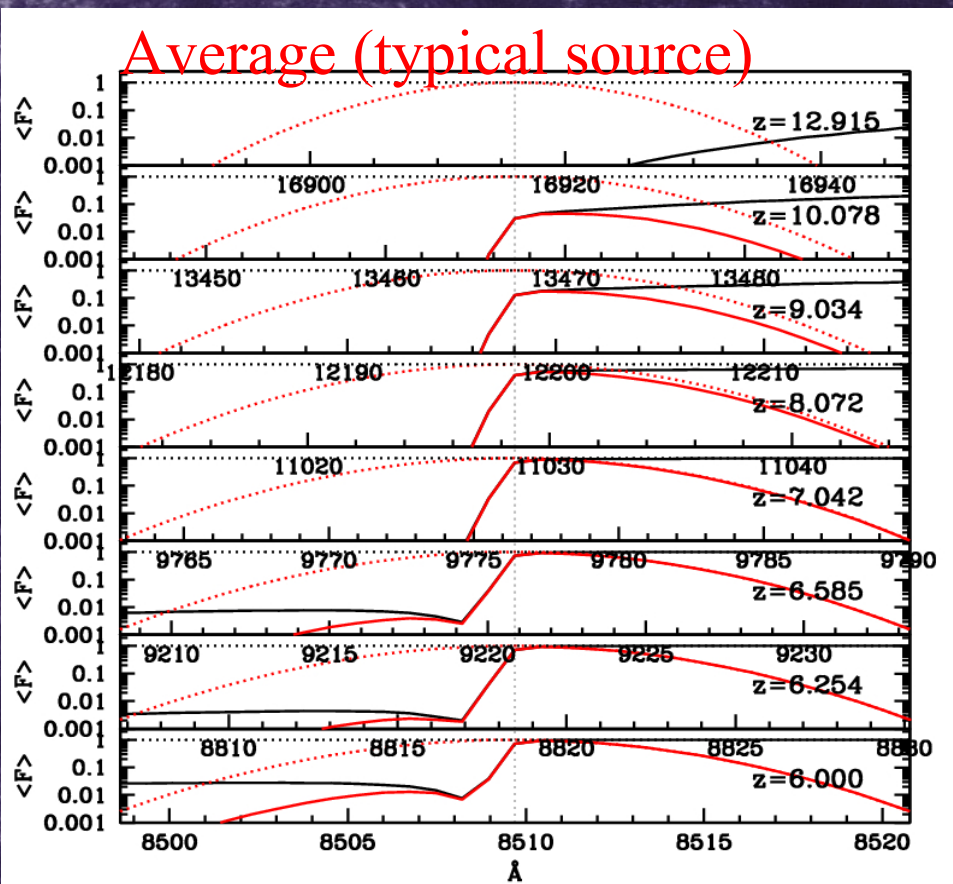
(Iliev et al. 2008, MNRAS, 391, 63)



Mean Ly- α line shape vs. z

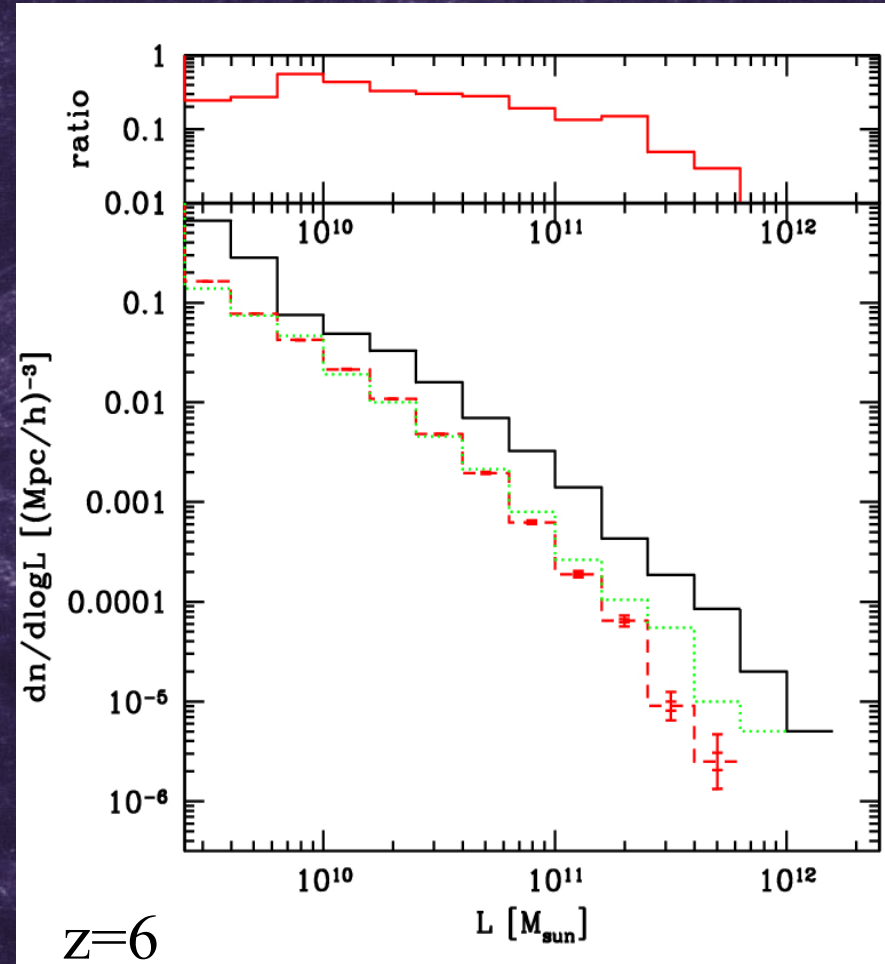
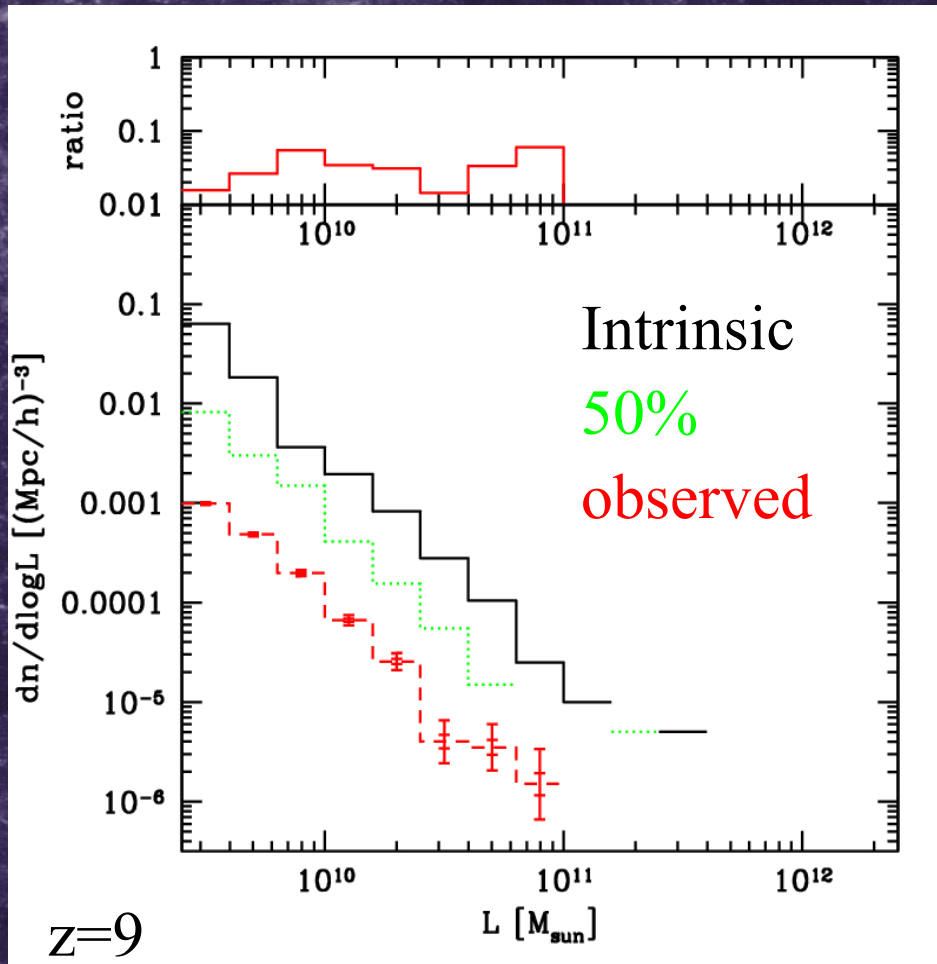
(Iliev et al. 2008, MNRAS, 391, 63)

- Mostly the red wing comes through (but damped at $z > 10$).
- Infall more important for luminous sources, changes the line shape.



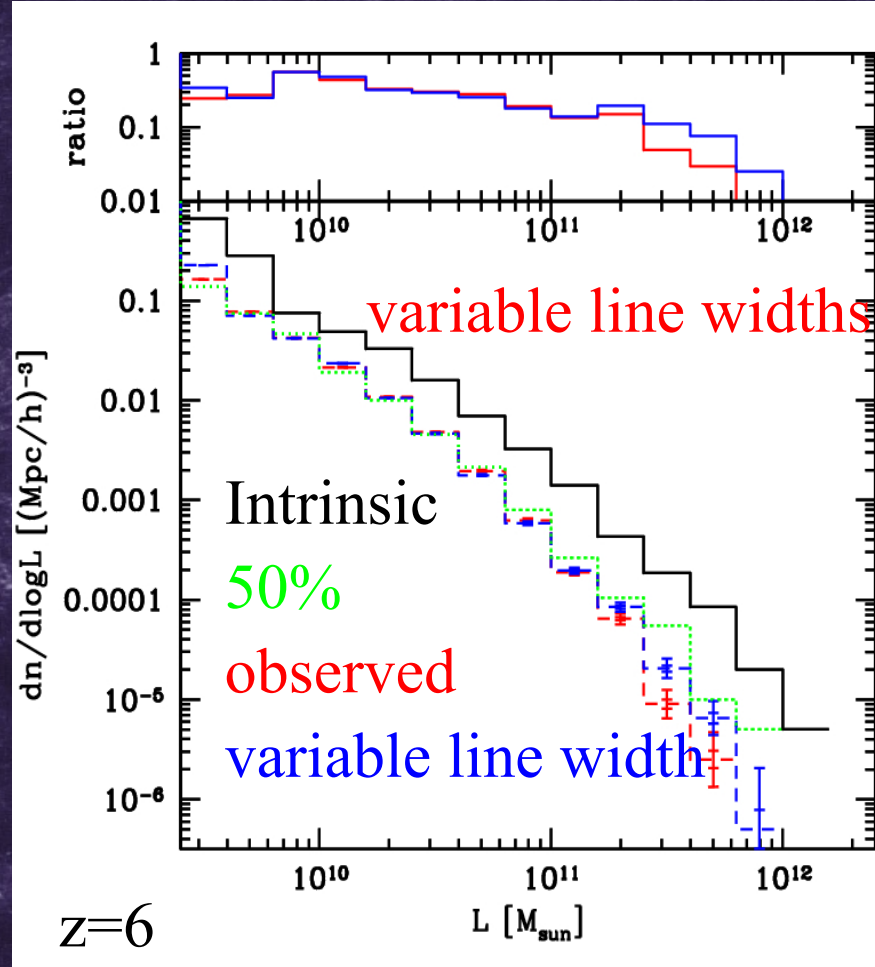
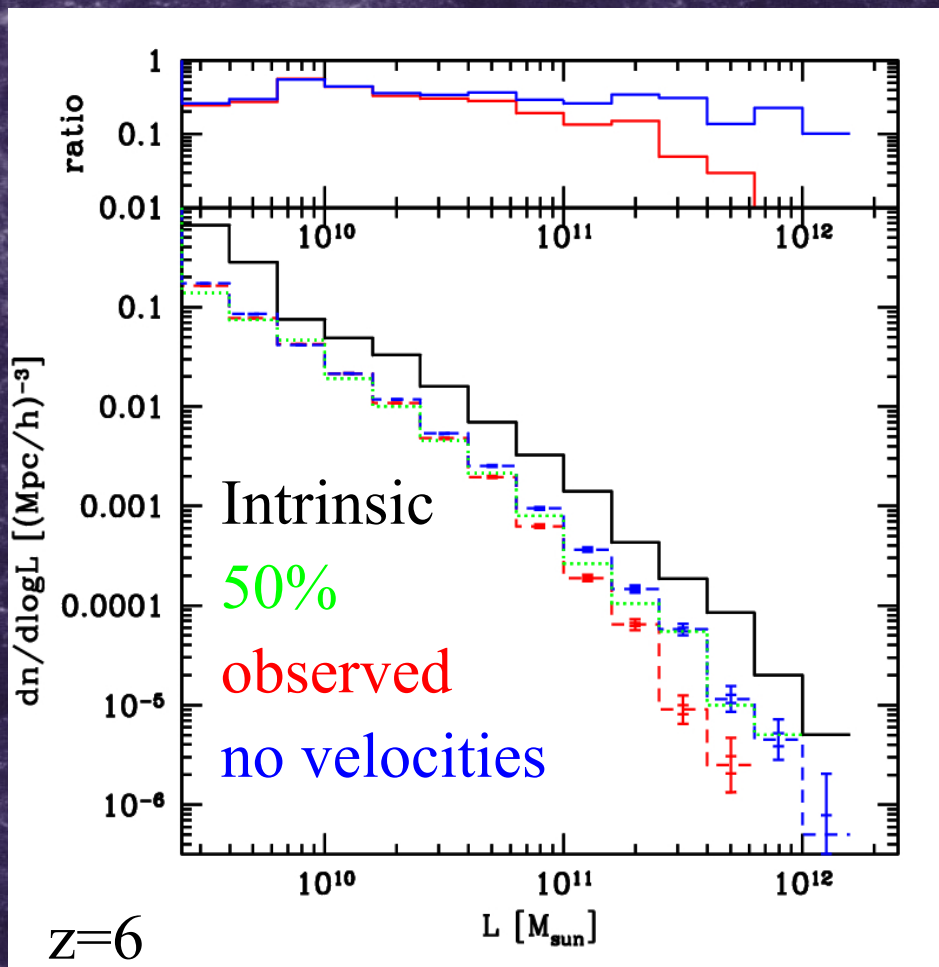
Ly- α Luminosity Functions

(Iliev et al. 2008, MNRAS, 391, 63)



Ly- α Luminosity Functions: effects of velocities and the assumed line widths

(Iliev et al. 2008 MNRAS, 391, 63)

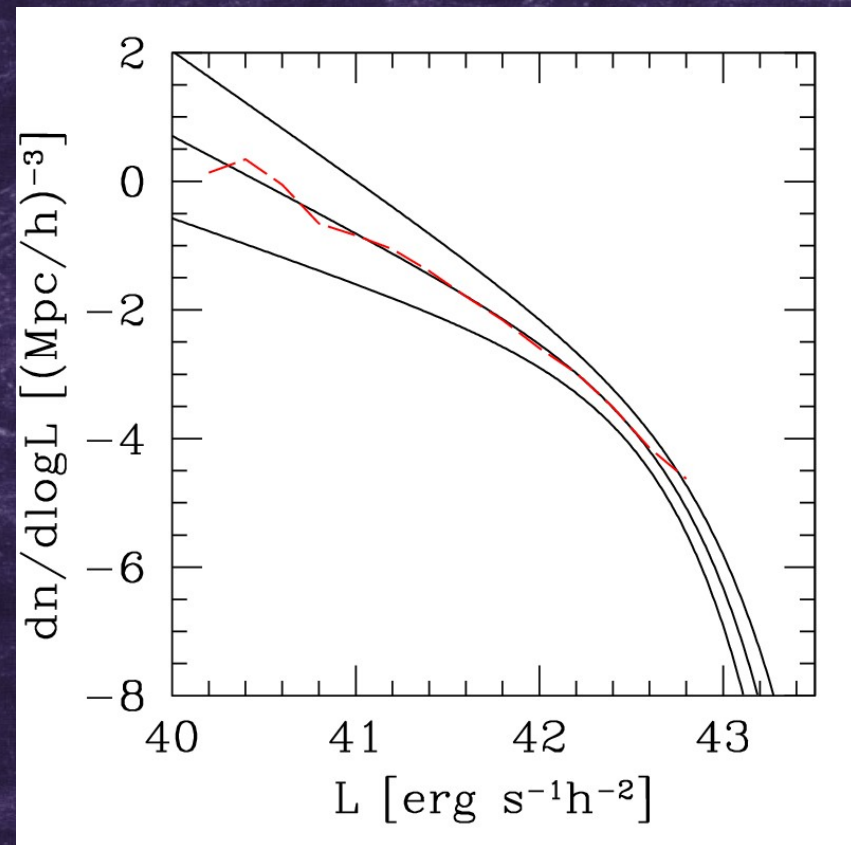


Luminosity function: simulations vs. observations

(Iliev et al. 2008, MNRAS, 391, 63)

LF normalization: set by matching the number density of sources in simulations to the observed one (by Kashikawa et al. 2006). Excellent match of the shape, for an assumed faint-end slope of -1.5 for the fit to the observations.

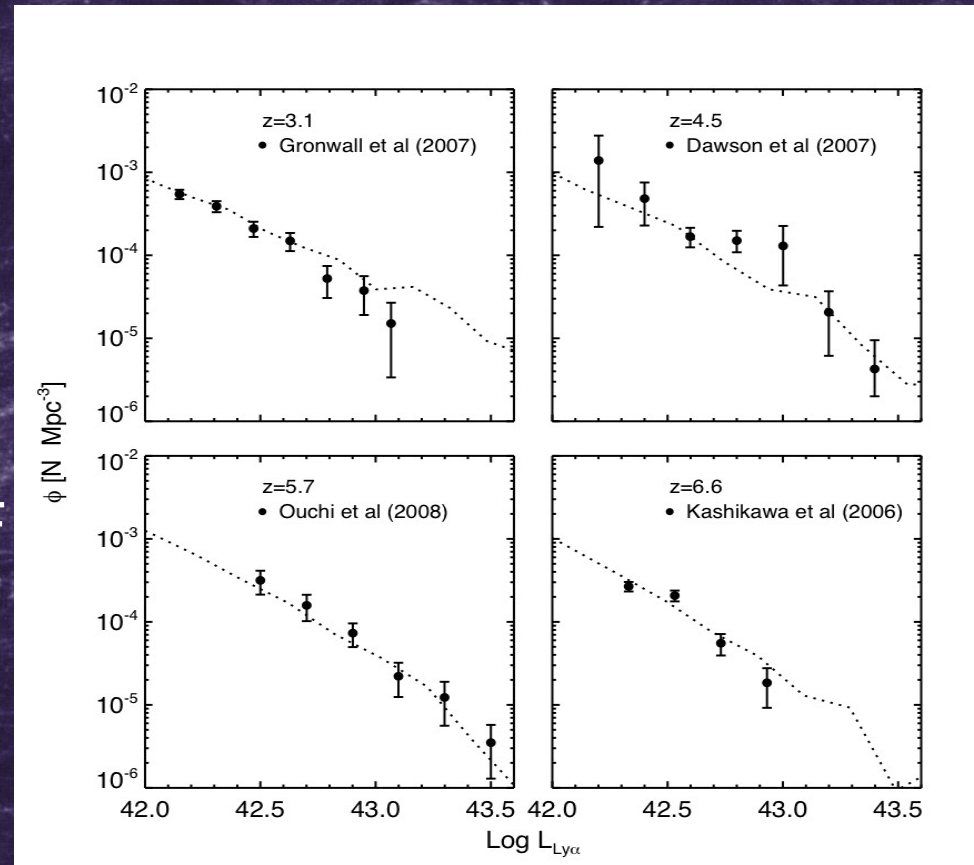
-> the **majority** of sources responsible for reionization are **too faint** to be observed at present.



A simple physical model for the luminosity function of Ly- α sources

(Tilvi, Malhotra, Rhoads, Scannapieco, Thacker, Iliev & Mellema, 2008, submitted, arXiv/0906.5159)

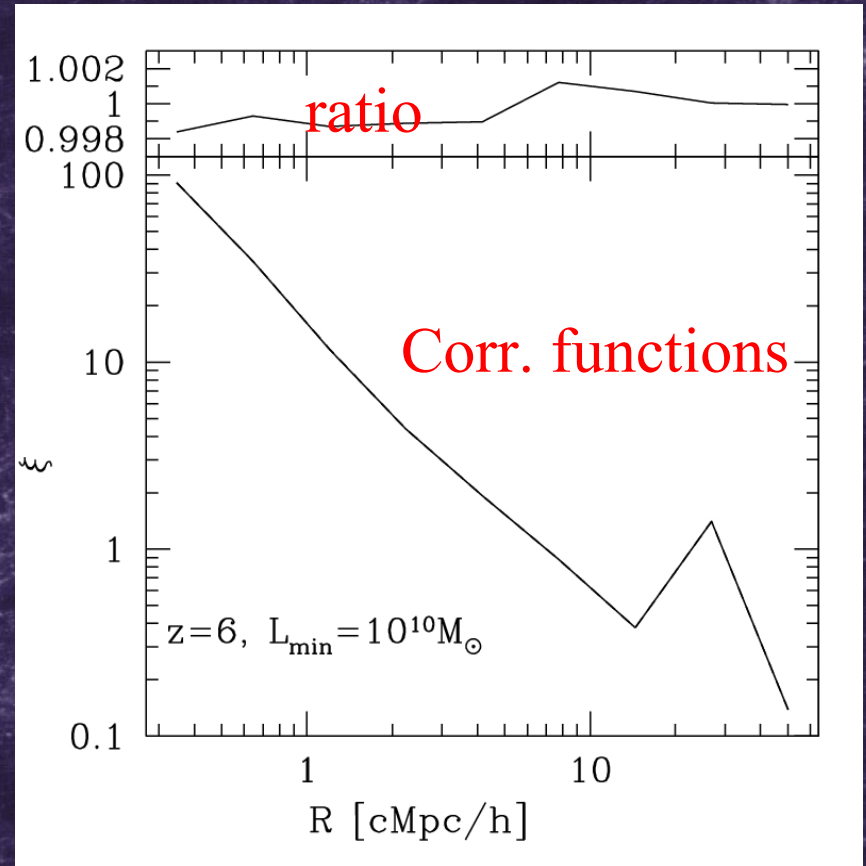
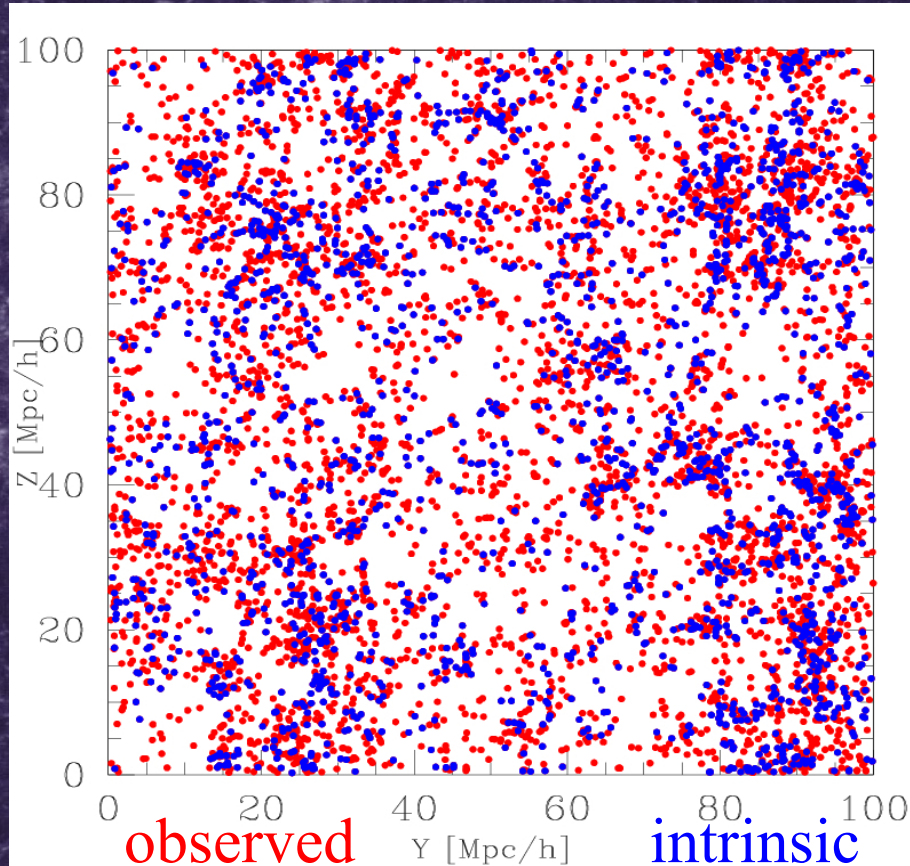
- A simple, 1-parameter model.
- Based on assumption that Ly- α luminosity is proportional to halo mass growth.
- Matches well the Ly- α LF data at $z=3-6.6$.
- Introduces naturally a duty cycle.
- Source clustering agrees well with observed one.



For more details see paper.

Correlation functions of Ly- α sources

(Iliev et al. 2008, MNRAS, 391, 63)

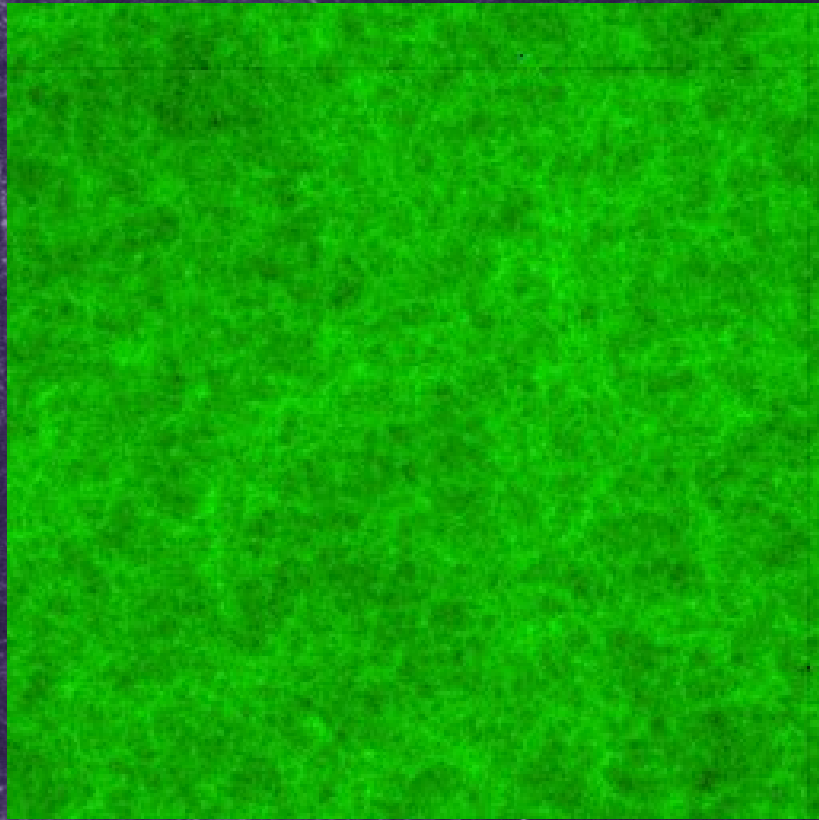


For a given (e.g. observed) **number density** of sources their clustering is largely **unaffected** by reionization patchiness (max 10% difference at small scales and at high- z , decreasing later).

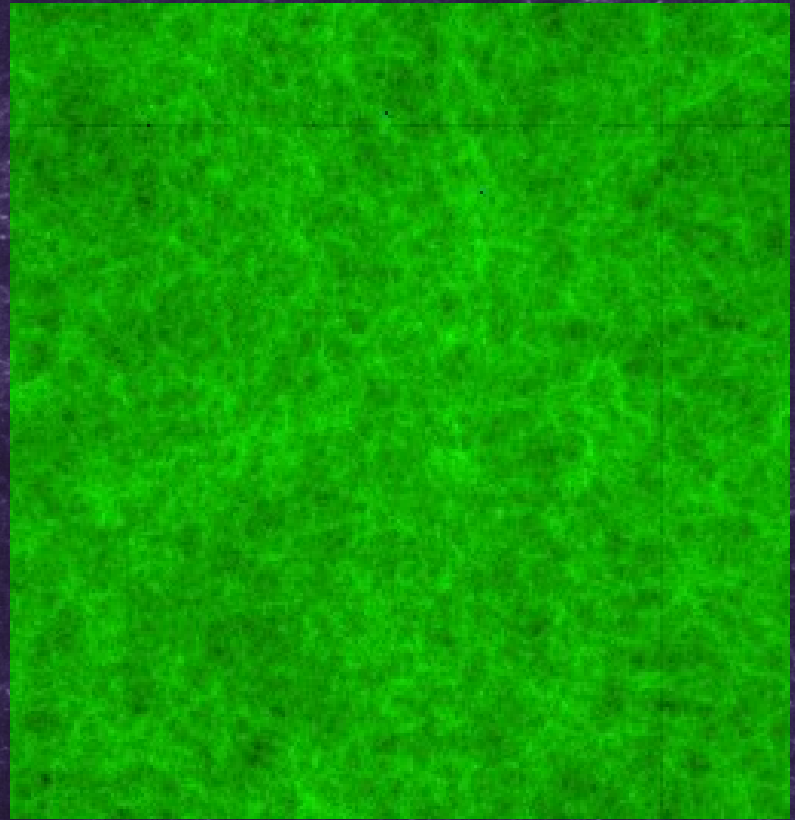
Reionization of the Local Group

(w/B. Moore, G. Yepes, S Goettlober, Y. Hoffman, G. Mellema;
work in progress)

Constrained simulations of the formation of the LG and its neighbourhood (GADGET, 64/h Mpc box, 1024^3 particles) post-processed with radiative transfer (on 256^3 grid), same method.



Milky Way



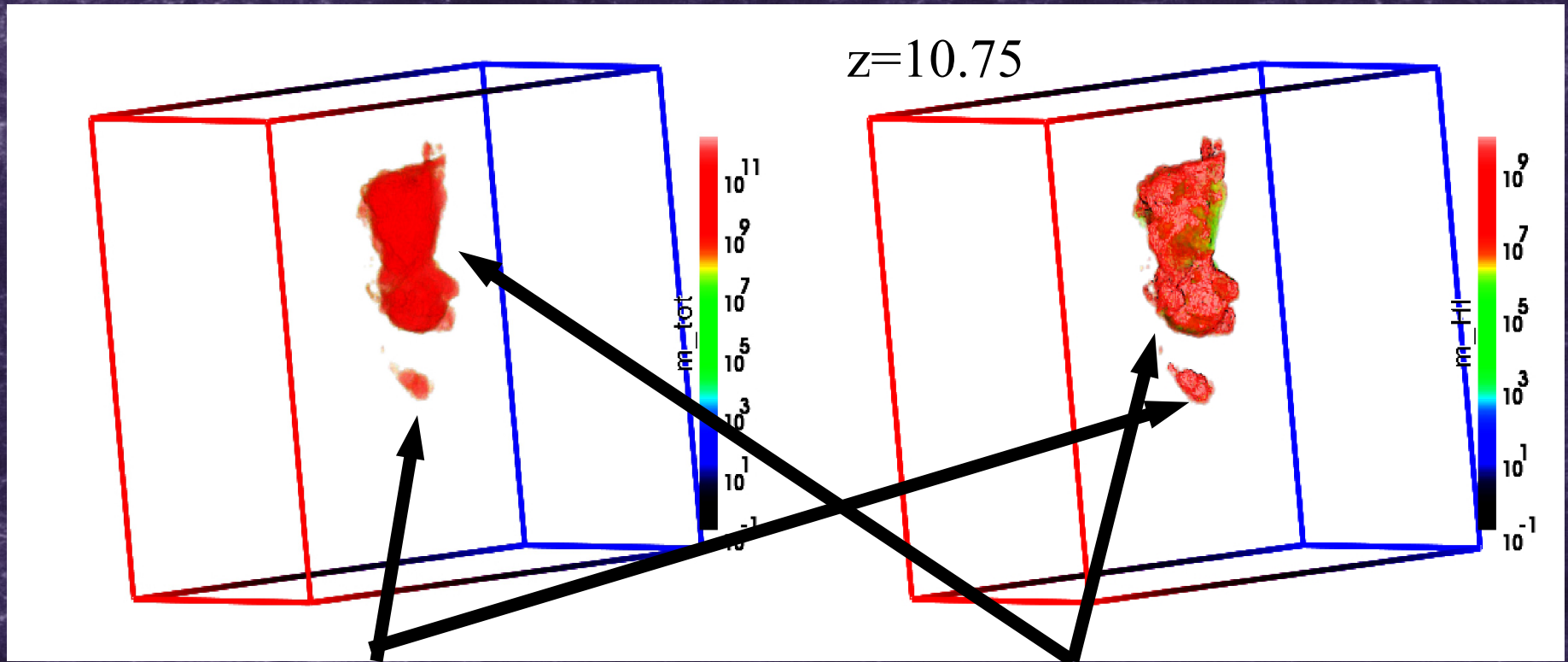
Virgo

Reionization of the Local Group: the evolution

Total mass

Neutral mass

$z=10.75$



(proto) Local Group

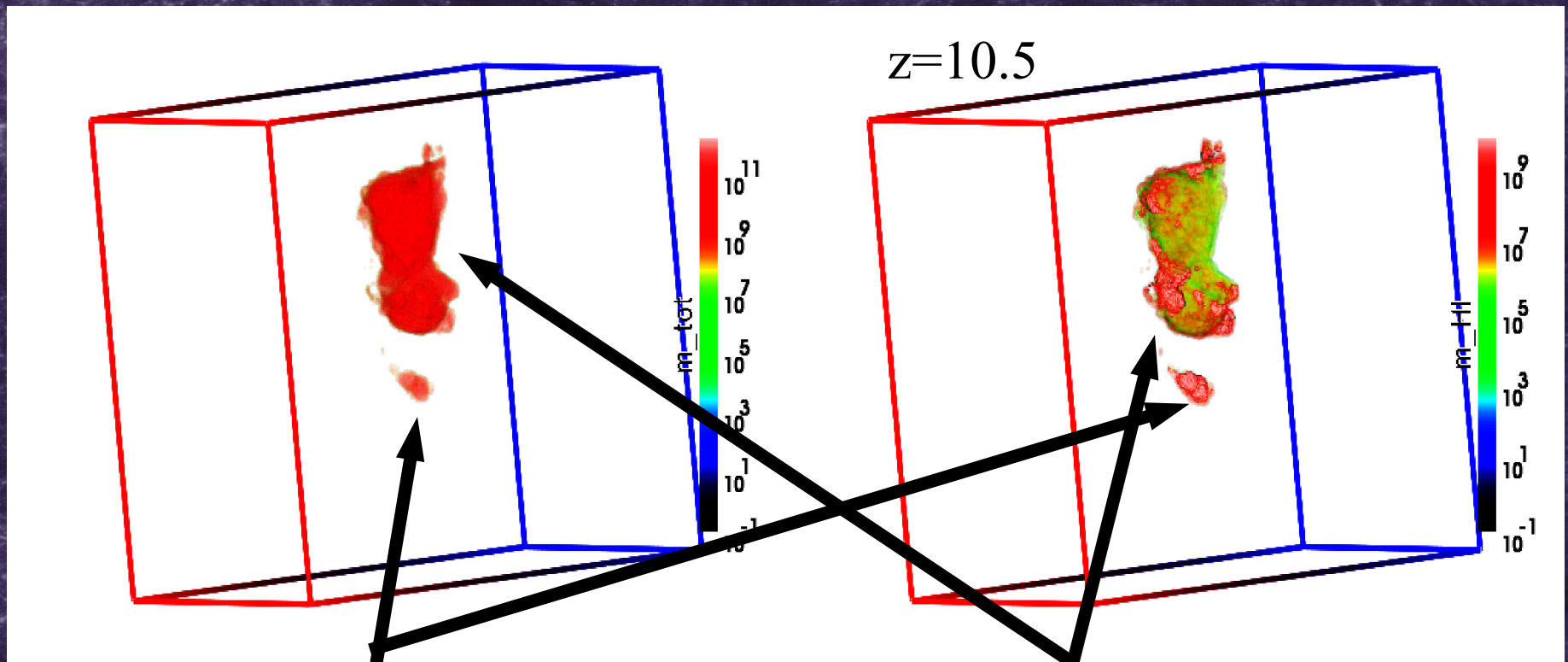
(proto) Virgo

Reionization of the Local Group: the evolution

Total mass

Neutral mass

$z=10.5$



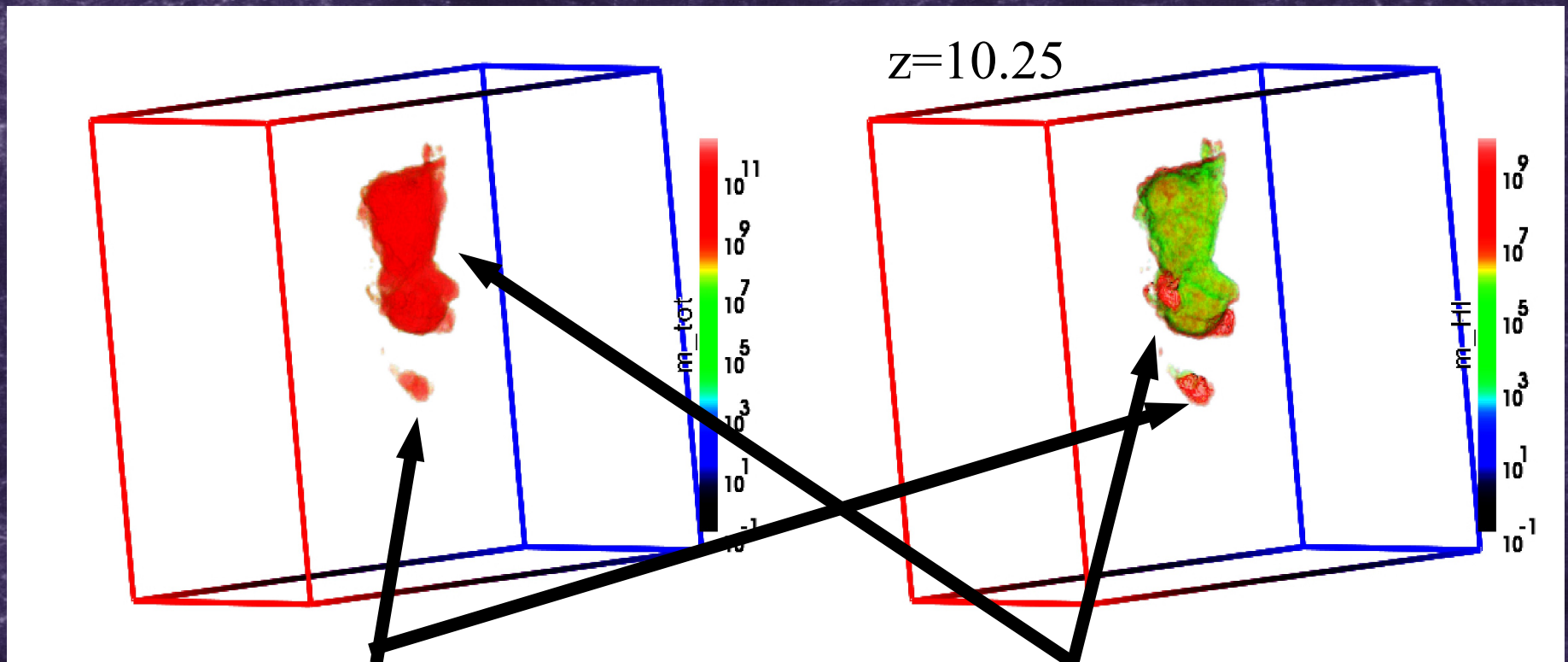
(proto) Local Group

(proto) Virgo

Reionization of the Local Group: the evolution

Total mass

Neutral mass



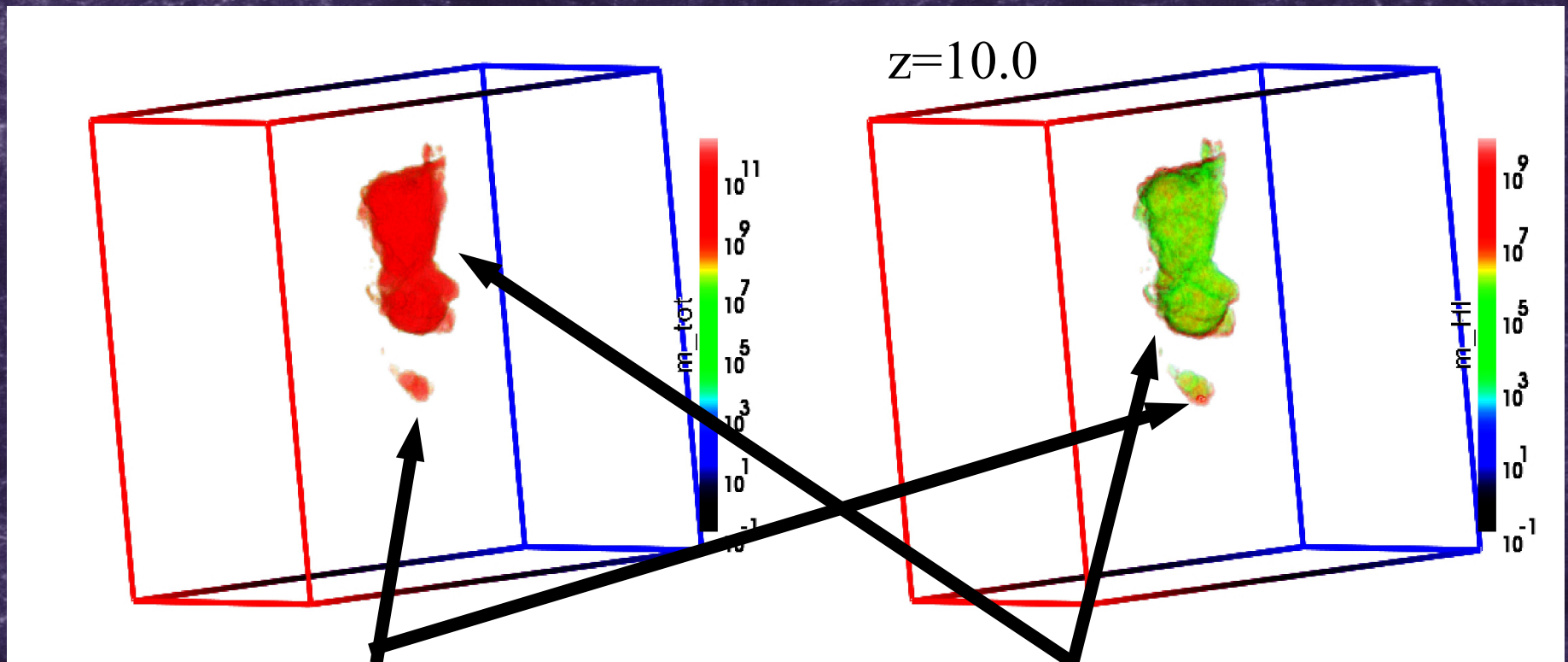
(proto) Local Group

(proto) Virgo

Reionization of the Local Group: the evolution

Total mass

Neutral mass

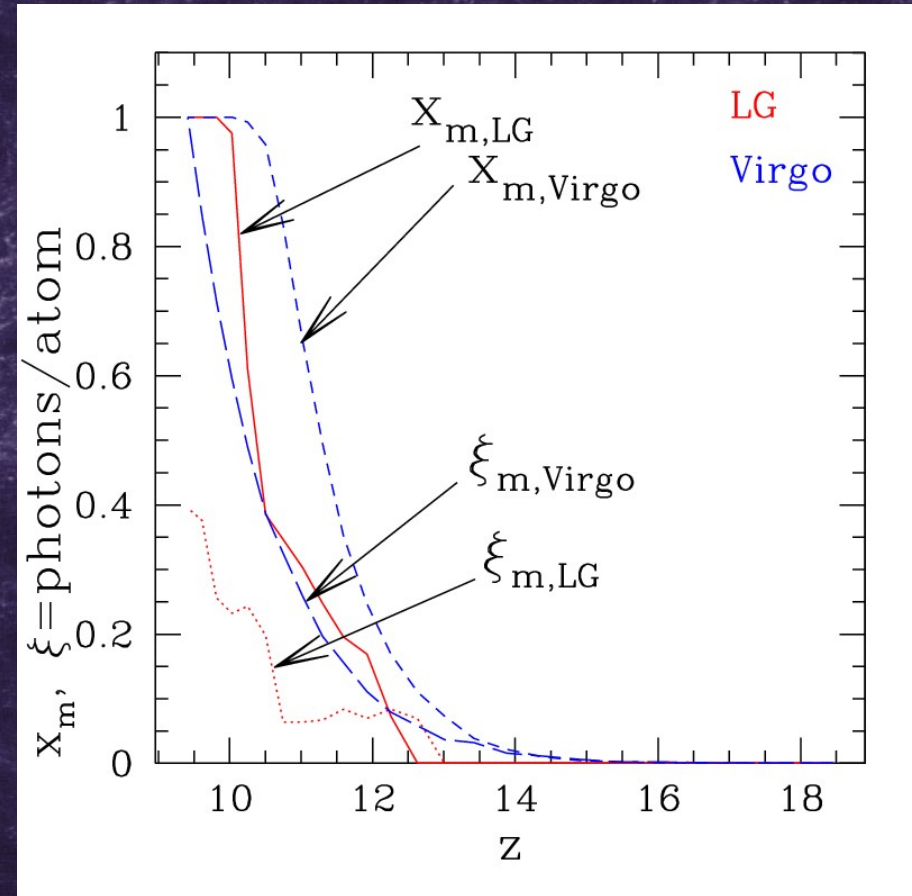


(proto) Local Group

(proto) Virgo

Reionization of the Local Group: the Photon Budget

- Both (pre-)LG and Virgo reionize at $z \sim 10$.
- At the time of LG reionization internal sources have produced just ~ 0.2 ionizing photons/atom \Rightarrow mostly **external** reionization
- Virgo constituents have produced ~ 0.6 photons/atom by $z \sim 10$ and 1 photon/atom by $z \sim 9.5$, i.e. its reionization is primarily, but not completely **internal**



Thank you for your attention!

Time for questions...